A Van Hove analysis of the reaction $(^{+})np(^{+})(^{-})(^{})at12GeV/C$

Alan Peter Lotts

A Van Hove

Analysis of the Reaction

$\pi^+ n \rightarrow p\pi^+\pi^-\pi^0$ at 12 GeV/C

A Thesis presented

by

Alan Peter Lotts

for the

Degree of Master of Science

at the

University of Durham

September 1973

ABSTRACT

This thesis contains an account of some of the work undertaken by the author while a member of the High Energy Nuclear Physics Group at the University of Durham. The first part of this thesis describes the procedures used to obtain a sample of events which correspond to a particular reaction channel. The data used was obtained from the results of an experiment using 12 GeV/c positive pions interacting in the C.E.R.N. Deuterium Bubble Chamber. The five laboratories which collaborated in the experiment were Durham, Genoa, Milano, LPHNE (Paris) and Ecole Polytechnique (Paris).

The second part of the thesis describes the application and results of a Van Hove analysis of the data sample. The analysis shows a good correlation between the predictions of simple Feynman diagrams and the events which populate the corresponding Van Hove regions.

The analysis proves useful for obtaining samples of events which contain particular low mass resonances. Amongst the resonances observed in the data sample are the ρ°, ρ^{+}, ω° and η° mesons and the $\Delta^{+}(1236)$ and $\Delta^{\circ}(1236)$ baryons.

CONTENTS

			Page
Abstract			i
Contents			ii
List of Figures and Tables			iv
Introduction			1
Chapter 1		Experimental Details and Event Selection	6
	1.1	The Exposure, Scanning and Measuring	6
	1.2	Fitting Events with the Programme GRIND	9
	1.3	Selection of Events from the Data Summary Tapes	12
	1.3.1	Introduction	12
	1.3.2	The Application and Results of the Selection Criteria	14
Chapter 2		The General Features of the Selected Data	19
	2.1	Technical Distributions	19
	2.2	Mass Distributions	21
Chapter 3		The Van Hove (L.P.S.) Method of Analysis	25
	3.1	Introduction	25
	3.2	Definition of Variables	28
	3.3	Definition of the Centre of Mass System	29
Chapter 4		The Results of L.P.S. Analysis	32
	4.1	Tripion Invariant Mass Spectrum in Region (1)	33
	4.2	The $M(p\pi^-)$ and $M(\pi^+\pi^0)$ Spectra in Region (2)	34

CONTENTS (Contd.)

		Page
4.3	The M($\rho\pi^0$) and M($\pi^+\pi^-$) Spectra in Region (4)	35
4.4	The M($\pi^+\pi^-$) Spectrum in Region (2)	35
4.5	Discussion of Dipion Spectra in Region (1)	36
4.6	The 'Δ' Signals in Region (5)	37
4.7	Conclusion	38
Conclusion		40
Appendix (A)		43
References		45
Acknowledgements		46

LIST OF FIGURES AND TABLES

Figure		Following Page
1 - 1	Probability Distribution before Selection (Durham Events only)	14
1 - 2(A)	Missing Mass Squared Distribution before Selection (Durham Events only)	15
1 - 2(B)	Missing Mass Squared Distribution after 10% Probability Selection	15
2 - 1	Probability Distribution	19
2 - 2	Missing Mass Squared Distribution	19
2 - 3(A) & (B)	Beam and Spectator Proton Momentum Distributions	19
2 - 3(C) & (D)	Angular Distribution of the Spectator Proton with respect to the beam for the Total Sample and for 4 Prongs alone	19
2 - 4	Momentum and Angular Distributions for the Fast Proton and the out-going pions	21
2 - 5(A)	Goldhaber Plot of $M(p\pi^0)$ / $M(\pi^+\pi^-)$	21
2 - 5(B)	Goldhaber Plot of $M(p\pi^-)$ / $M(\pi^+\pi^0)$	21
2 - 6(A)	Invariant Mass Distribution of $(p\pi^0)$	22
2 - 6(B)	Invariant Mass Distribution of $(\pi^+\pi^-)$	22
2 - 6(C)	Invariant Mass Distribution of $(\pi^+\pi^-)$, Four Prongs only	22
2 - 7(A)	Invariant Mass Distribution of $(p\pi^-)$	23
2 - 7(B)	Invariant Mass Distribution of $(\pi^+\pi^0)$	23
2 - 7(C)	Invariant Mass Distribution of $(\pi^+\pi^0)$, Four Prongs only	23
2 - 8(A)	Invariant Mass Distribution of $(\pi^+\pi^-\pi^0)$	23
2 - 8(B)	Invariant Mass Distribution of $(\pi^+\pi^-\pi^0)$, Four Prongs only	23

LIST OF FIGURES AND TABLES (cont.)

Figure		Following Page
2 - 8(C)	Invariant Mass Distribution of $(\pi^-\pi^\circ)$	23
3 - 1	The L.P.S. Cuboctahedron and the Equations for a 4 body Van Hove Analysis	28
4 - 1	Peyrou Plots for the Fast Proton and the three outgoing pions	32
4 - 2	Scatter Plot of θ_1 / θ_2	32
4 - 3	The Invariant Mass Distribution of $(\pi^+\pi^-\pi^\circ)$ for Region 1	33
4 - 4(A)	The Invariant Mass Distribution of $(p\pi^-)$ for Region 2	34
4 - 4(B)	The Invariant Mass Distribution of $(\pi^+\pi^\circ)$ for Region 2	34
4 - 5(A)	The Invariant Mass Distribution of $(p\pi^\circ)$ for Region 4	35
4 - 5(B)	The Invariant Mass Distribution of $(\pi^+\pi^-)$ for Region 4	35
4 - 6(A)	The Invariant Mass Distribution of $(\pi^+\pi^-)$ for Region 2, the best resonance signal in an 'incorrect' Region	36
4 - 6(B), (C), (D)	The Dipion Invariant Mass Distributions for Region 1	36
4 - 7	Scatter plot of $M(p\pi^-)/M(p\pi^\circ)$ for Region 5, 'leading pion' events	37
Table 1	Selection Statistics	17
Table 2	Three Prong 'errors'	44

INTRODUCTION

For several decades considerable interest and effort has been expended in understanding strong interactions and the properties of the elementary particles that result from such interactions.

With the advent of high energy accelerators, controlled beams of elementary particles became available in the laboratory which facilitate detailed studies of strong interactions. The bubble chamber used in conjunction with an accelerator produced beam has been one of the most fruitful techniques in this area of physics. The great advantage of the bubble chamber is that the target medium also acts as the detecting system to give a visual record of the nuclear interactions occurring in the chamber which can be measured with considerable precision over the whole 4π solid angle.

Although accelerator beams of most types of "stable" elementary particles are available the charge pion beam has been most used due to the relative ease of production and also because its use in conjunction with a bubble chamber allows the investigation of the pion-nucleon interaction which is fundamental to the understanding of strong interactions.

A great deal of work has already been performed

on the pion-proton system using hydrogen filled bubble chambers and many elementary particle states have been observed resulting from this system. However, the neutron is also a nucleon and it would be advantageous to have data on the pion-neutron interaction to complement the data on the pion-proton interaction.

It is more difficult to provide a neutron target for a pion beam and the normal method is to use a deuterium filled bubble chamber and then to select the events corresponding to a pion-neutron interaction. It is fortunate that in the visual record of the interation of pions with deuterium it is a relatively easy task to recognise pion-neutron interactions in the presence of the other possible interactions (pion-proton, pion-deuteron).

The work in this thesis describes the selection of events corresponding to pion-neutron interactions from an experiment where a deuterium filled bubble chamber has been exposed to a positive pion beam of momentum of 11.7 GeV/c. The particular interaction investigated is the reaction $\pi^+ d \rightarrow p_s p \pi^+ \pi^- \pi^0$ where, by demanding that the final state nucleon is a proton, the mesonic system is constrained to be of zero overall charge.

In this reaction $\Delta^{++}(1236)$ production is expected to be small as the reaction resulting in such a state can only proceed by an exotic T=2 exchange or by

baryon exchange. Thus from an initial $\pi^+ n$ state, $\Delta^{++}(1236)$ cannot be produced by the usual exchange processes, whereas production of this isobar is possible by meson exchange from a $\pi^+ p$ initial state. Consequently the final state in a $\pi^+ n$ experiment is expected to be more dominated by the formation of mesonic resonances in the dipion and tripion systems than a comparison with a similar $\pi^+ p$ experiment would suggest.

The tripion system in the reaction being studied here has an overall charge of zero but contains two charged pions. The charge symmetric reaction, which has a $\pi^- p$ initial state, can also result in a neutral tripion final state similar to the system being reported in this thesis. However the charge symmetric reaction implies both a fast neutron and a neutral pion in the final state and since only charged particles leave visible tracks in a bubble chamber this reaction is considerably more difficult to study. Other initial states can also produce a neutral tripion system but only as a subset of a four (or more) pion system.

The above deuterium reaction allows the investigation of both neutral dipion systems and neutral tripion systems in the same reaction channel and since every mesonic resonance has a neutral decay mode, contributions could be expected from all resonances which decay to two or

three pions within the accessible energy range of the experiment.

One partial disadvantage of the $\pi^+ n$ initial state is that it is a mixed isospin state, containing both T=1/2 and T=3/2 components. This makes some calculations more difficult as compared with a pure isospin initial state such as $\pi^+ p$.

Thus a modest statistics $\pi^+ n$ experiment is perhaps more rewarding for a study of neutral dipion and tripion systems than a higher statistics experiment using any other of the more common initial states.

A brief description of the exposure, scanning and measuring associated with the experiment is given in Chapter 1, which also contains details of the selection procedures used to obtain a sample of events corresponding to the above deuterium reaction (referred to as reaction 2A). Some general features of the selected data are presented in Chapter 2. These include the momentum and angular distributions of the interacting particles in the laboratory system as well as the Missing Mass squared and probability distributions of the selected events. The invariant mass spectra for the various combinations of particles are also displayed and discussed in Chapter 2, prior to the use of the Van Hove method of analysis, the results of which are presented in Chapter 4. Chapter 3 includes a description of Van Hove analysis together with the

definitions of the centre of momentum system and the variables needed for a Van Hove analysis of four body final state data.

CHAPTER 1

EXPERIMENTAL DETAILS AND EVENT SELECTION

1.1 The Exposure, Scanning and Measuring

The exposure was performed at the CERN Proton Synchrotron in late 1967. The CERN 2m Bubble Chamber filled with deuterium was used in conjunction with the U3 beam line which produced positive pions of nominal momentum 11.7 GeV/c. The U3 beam line (Ref.1,2) contained two Radio Frequency Separators for mass resolution. It has been calculated that the contamination of the beam by K^+ particles was less than 1% (Ref.2).

A total of 150K pictures were taken in two separate runs. The films were distributed amongst the collaborating laboratories, Durham, Genoa, Milano, LPHNE (Paris) and Ecole Polytechnique (Paris) for scanning, measuring and processing of the data.

The films were scanned for all types of events which had up to ten prongs. It was decided after scanning to concentrate initially on the events that might belong to the following reactions:-

$$\pi^+ d \rightarrow d\,\pi^+\pi^+\pi^- \qquad (1)$$

$$\pi^+ d \rightarrow d\,\pi^+\pi^+\pi^-\pi^0 \qquad (1A)$$

$$\pi^+ d \rightarrow p_s\, p\, \pi^+ \pi^- \qquad (2)$$

$$\pi^+ d \rightarrow p_s\, p\, \pi^+ \pi^- \pi^0 \qquad (2A)$$

(See Ref. 3 for published papers on these reactions)

Other reactions involving strange particles are also possible; however, the total cross-section for strange particle production is very small and these have not been considered further.

All four prong non-strange events with a stopping track or a candidate proton track were selected for measurement along with all three prong non-strange events. A strange event is defined as one with an associated V^0 or a 'kinked' track. A three prong event corresponds to an interaction where the deuteron or spectator proton has insufficient momentum to give a visible track, (i.e. has a range $\leq$ 1mm in chamber space). It should be noted that if the incoming pion interacts with the proton of a deuteron, conservation of charge in the interaction implies that it can only result in an even prong final state.

If the interaction is between the incident pion and the neutron in the deuteron while the proton is not involved in the interaction, then the proton is called the spectator proton. The spectator proton, after the interaction, will, in the impulse approximation, have the momentum that it had initially while within the deuteron, and this is described by the Hulthen wave function for the deuteron. In general, the spectator momentum will

be small and in approximately two thirds of the cases it will have insufficient momentum to leave a visible track in the bubble chamber. Obviously a large fraction of the events selected for measurement will have a spectator proton and will belong to one of the following reactions:-

$$\pi^+ n \rightarrow p \pi^+ \pi^- \qquad (2)$$

$$\pi^+ n \rightarrow p \pi^+ \pi^- \pi^0 \qquad (2A)$$

The selected events were measured on convential film plane digitized machines and processed through the THRESH-GRIND programme system.

THRESH is a three view geometrical reconstruction programme. It uses the two dimensional measurements from each view to reconstruct an event in three dimensions. The output includes the positions of vertices together with the radius of curvature, direction and measured length of each track in an event. Estimates of the errors associated with this information are also included.

GRIND is a kinematic fitting programme which uses THRESH output. The measured curvatures of tracks (when available) are converted into momenta using the known characteristics of the magnetic field within the chamber and then fits to user supplied hypotheses are attempted. The four equations to be satisfied in the fit to an event are called the constraint equations and require momentum conservation (in three dimensions) and

energy conservation. GRIND calculates the 'external' errors for each track using only the length of the track from THRESH and combining this with standard estimates of the measuring accuracy. A comparison is then made between these 'external' errors and the 'internal' erros calculated by THRESH when reconstructing the tracks. For a further discussion of 'internal' and 'external' errors, see Ref. 4. The 'external' errors are used in the GRIND fitting process although, when a fit is possible, a new set of error estimates (called the fitted errors) are calculated, as well as the fitted parameters of the fit. The chi-squared and number of degrees of freedom of the fit are also calculated which enables the probability of the fit to be estimated.

1.2 Fitting Events with the Programme GRIND

Ignoring for the moment the problem of the spectator proton, when GRIND attempts to fit a hypothesis to a reconstructed event, there are three possible results:-

(1) A 4 constraint fit (4c)

(2) A 1c fit

(3) A no-fit

A 4c fit will occur if it is not necessary to include a neutral particle in order to obtain a fit. This implies that there are no complete unknowns in the

four constraint equations to be satisfied, i.e. the problem is over determined. For a particular event it is therefore possible to calculate a set of fitted parameters which will have considerably smaller errors than the 'external' errors would suggest.

The 4c fit thus represents the best possible fit to this type of bubble chamber data since the only assumptions it is necessary to make are the masses of the particles producing the seen tracks in the bubble chamber, and it is always necessary to make these assumptions.

A 1c fit will occur if a fit can be obtained when it is assumed that only one neutral particle (usually a neutral pion) is missing. Once the mass of the missing particle is assumed there are four constraint equations to be satisfied with only three unknowns (the p, λ, ϕ of the missing particle) and hence a solution is still possible. Since the measured values do have errors however, there is considerably less error reduction resulting from a 1c fit as compared with a 4c fit, and so it is usual to reject 1c fits in favour of a 4c fit to the same event, even though the probability given to the 1c fit may be higher. Some justification for the preference of any 4c as compared with a 1c fit can be obtained by the use of a programme such as FAKE. This programme uses random numbers to generate specific types of event which can then be fitted by the usual

procedures. The results obtained by using FAKE and then GRIND suggest that while a generated 4c 'event' can frequently give a 1c fit as well as the expected 4c fit, a generated 1c event will rarely produce an associated 4c fit.

A no-fit effectively occurs when the resultant probability of all 4c and 1c fits attempted by GRIND is very small, although in many cases no fit of any kind can be found. This usually implies that more than one neutral (unseen) particle was produced in the interation and so the only information available about the event is the measured values for the tracks and hence the total energy and momentum of the unseen particles. These values of Missing Energy and Missing Momentum enable the effective Missing Mass of the unseen particles to be calculated. No-fit events represent the largest part of the data available in this experiment.

The four prong events were processed quite normally through the GRIND fitting programme. However, in the case of the three prong events where the spectator proton (or deuteron) is unseen, GRIND had to be modified before fits to these events were possible. When attempting to fit with a missing deuteron, the deuteron was treated as completely unseen and so a 1c fit resulted (reaction 1). Obviously it was not possible to fit both a missing deuteron and a missing neutral pion to a three prong event and so fits to reaction 1a

were not attempted.

When fits to reactions 2 and 2A were attempted for three prong events, it was necessary to assume that the missing particle was a spectator proton. It will then have a momentum distribution given by the Hulthen wave function, and so, although unseen, some information about the nucleon is available, i.e. the momentum is $\leq$ 90 MeV/c. These missing protons were included in the fit via the ZEROL routine in GRIND where the fit is initiated with the spectator proton having:-

$$P_x = P_y = P_z = 0$$

$$\Delta P_x = \Delta P_y = 30 \text{ MeV/c} \quad , \quad \Delta P_z = 42 \text{ MeV/c}$$

Fits to both reaction 2 and 2A are then possible. The validity of this approach can be confirmed by comparing the fitted spectator proton momentum distribution with that predicted by the Hulthen wave function.

The GRIND output was correlated with the ionisation of the tracks as seen on the scanning table and those fits compatible with ionisation were included on a Data Summary Tape (DST). The DST of each laboratory was circulated to the other laboratories in the collaboration for analysis.

1.3 Selection of Events from the Data Summary Tapes (DSTs)

1.3.1 Introduction

These sections give details of the selection procedures used to extract from the DSTs a sample of events which should contain the highest possible proportion of unambiguous fits to the reaction 2A.

The main parameters of a fit to an event given by GRIND are:-

1. The probability of the fit.
2. The Missing Mass Squared. This includes any fitted neutral but does not include an unseen spectator proton.
3. The error on the Missing Mass Squared.
4. The Missing Energy together with its error.
5. The momentum and direction of all the fitted particles with errors.

Since fits to reaction 2A fall in the 1c category, it is expected that considerable ambiguity will be present in the basic DST data. Ambiguity occurs when GRIND gives fits to more than one reaction for a particular event. This is due to:-

1. The intrinsic measurement accuracy.
2. Misidentification of tracks in the final state.

The number of events fitting due to measurement errors can be reduced considerably by suitable event selection criteria.

Misidentification of tracks can only occur between the proton and a positive pion in the final state and this is normally eliminated by checking the ionisation of the tracks on the scanning table. This procedure is increasingly efficient for proton momenta below about 1.5 GeV/c and is totally effective at about 1.2 GeV/c.

As the initial sample contained only about 7,000 fits some care is needed in making selections in that a balance is needed between producing a very pure sample with low statistics and a heavily contaminated sample with higher statistics.

1.3.2 The Application and Results of the Selection Criteria.

The initial selection was made on the probability of the fits. Before any selection was made, the distribution of the probabilities (shown in Fig. 1-1, for Durham events only) was peaked towards zero and, as all probabilities should be equally likely, it is clear that many of the lower probability fits were not true 1c events. From the slope of the distribution it was decided that a selection in probability at 10% would have the best decontamination effect while still preserving reasonable statistics.

The next selection was made on the Missing Mass

FIGURE 1-1

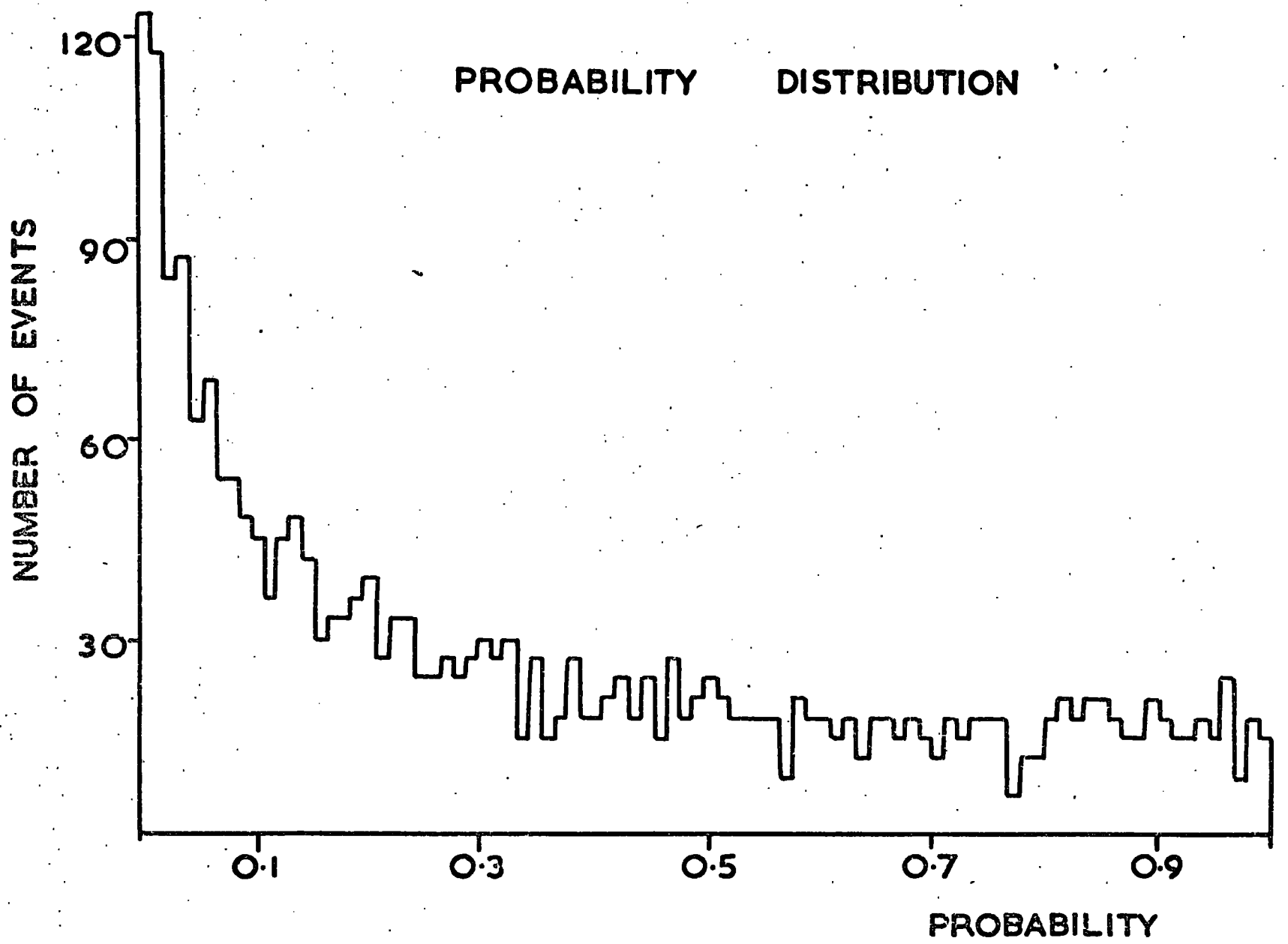
PROBABILITY DISTRIBUTION
NUMBER OF EVENTS
120
90
60
30
0·1
0·3
0·5
0·7
0·9
PROBABILITY

squared distribution. Fig. 1-2(A) shows the Missing Mass squared distribution for Durham events only, before any selection. (The other laboratories' distributions for Fig. 1-1 and 1-2(A) are very similar).

For a 1-π^0 fit one would expect a distribution of Missing Mass squared values centred on 0.02 $(GeV/c^2)^2$ and with a width determined by the experimental errors. However, as can be seen in Fig. 1-2(B), the distribution of Missing Mass squared values, after the 10% probability cut, is centred near zero, with an excess in the positive values. The mode of the Missing Mass squared distribution is compatible with 0.02 $(GeV/c^2)^2$ ($M(\pi^0)^2$). The excess of high positive Missing Mass squared values however, all had large errors which enabled them to give a one π^0 fit. These events could possibly have two or more π^0 s.

With this in mind a selection was designed to make the Missing Mass squared MM^2 distribution symetric, since in general only measurement errors should contribute to the negative Missing Mass squared values. The actual selection used was:-

The event was accepted if

$$MM^2 - \Delta MM^2 < 0.1 \ (GeV/c^2)^2$$

where ΔMM is the error on the Missing Mass squared value.

A straight-forward selection on the Missing Mass

FIGURE 1-2

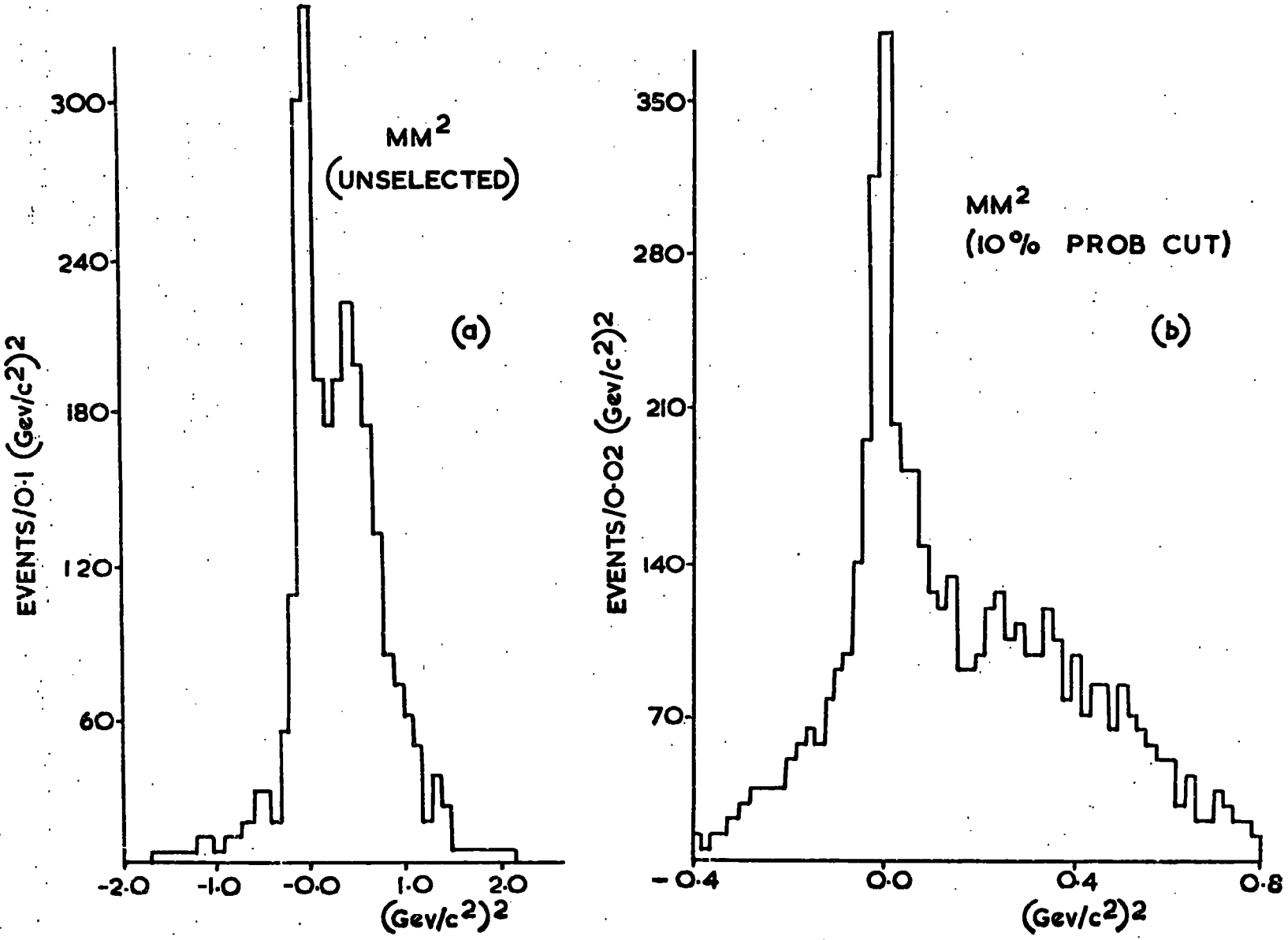
MM²
(UNSELECTED)
(a)
EVENTS/0·1 (Gev/c²)²
300
240
180
120
60
-2·0
-1·0
-0·0
1·0
2·0
(Gev/c²)²
MM²
(10% PROB CUT)
(b)
EVENTS/0·02 (Gev/c²)²
350
280
210
140
70
-0·4
0·0
0·4
0·8
(Gev/c²)²

squared values, or a selection on the errors, involved a large loss in statistics for a similar effect.

The next selection used was intended to eliminate the proton/pion ambiguity. This involves rejecting all fits where there is a fast proton with a fitted momentum in excess of 1.2 GeV/c. At a proton momentum of 1.2 GeV/c the density of bubbles of the track of a proton is clearly distinguishable from the track of a pion because the ionisation rate of a proton at this momentum is approximately 1.5 times larger than that of a pion. Thus protons and pions can be identified unambiguously from the track density for a momentum of less than 1.2 GeV/c. The effect of this selection is to remove many of the possible ambiguities, not only within the channel but also with other channels. Within the channel the ambiguity arises when two positive tracks can be fitted as either proton/pion or pion/proton respectively.

Using the final sample to give the proton momentum distribution and fitting an exponential function to the falling tail of this distribution, it is predicted that the number of events lost by the momentum selection is approximately 10%.

The final selection simply removed all 1c fits where a 4c fit occurred for the same event. This was done simply because even a low probability 4c fit is

much more likely to be the true fit to an event than a 1c fit.

The results of these selections are tabulated in Table 1. The first column shows the number of fits rejected by each of the selections acting alone on the sample. The second shows the number rejected by each selection when the selections were used in sequence while the third column gives the total kept after each sequential selection.

To verify the validity of the selections described above, the various mass distributions of the final state particles for the rejected events have been examined. As would be expected, there is resonance production in some combinations of the seen charged particles, (e.g. ρ^0 and Δ^0 production, but little evidence for resonance production when the unseen π^0 is combined with the seen particles (e.g. there is no ω^0 signal). However, 1c fits which are ambiguous with 4c fits appear to give low mass enhancements in the $\pi^+\pi^0$ and $p\pi^0$ systems. Since the majority of these 4c fits are of acceptable probability, it is reasonable to exclude these events from the sample of rejected 1c fits in order to determine the effects of the other selections. When the 4c ambiguities are removed, both the $\pi^+\pi^0$ and $p\pi^0$ mass distributions show no significant enhancements.

These selections give a final sample of about 2,000 events. The fact that many fits were rejected by only one selection suggests that all the selections were

TABLE 1

Statistics of the Selection of a Final Sample of 2023 Events from an Initial Sample of 7661 Fits

Statistics / Selection	No. of Fits Kept	No. of Fits Rejected	No. of Fits After Selection
Probability Selection at 10%	5494	2167	5494
Missing Mass Selection	4905	921	4573
Fast Proton Momentum Selection	3638	2031	2542
1c/4c Ambiguity Selection	6963	519	2023

Number of Fits Rejected by 1 Selection	2796
" " " " " 2 "	1608
" " " " " 3 "	1224
" " " " " 4 "	10

necessary.

This number of events represents about 70% of the eventual sample since some data within the collaboration is not yet available.

CHAPTER 2

THE GENERAL FEATURES OF THE SELECTED DATA

This chapter is intended to show the overall features of the data before a more detailed analysis is presented. All the figures in this chapter contain the fitted data of the final sample without any selections other than those described in the previous chapter.

2.1. Technical Distributions

The probability distribution, shown in Fig. 2-1 is isotropic as expected. However, since the actual Missing Mass distribution (Fig. 2-2) is still slightly assymetric, it would appear that the Missing Mass selection used is a reasonable compromise between the factors involved, since a more severe Missing Mass selection produces an anisotropic distribution of probabilities.

The fitted momentum distributions of the beam and spectator proton are shown in Fig. 2-3 (A) and (B), together with the angular distributions of the spectator with respect to the beam for the total sample and for the four prong events alone (Fig. 2-3 (C) and (D)). The twin peaks of the beam momentum represent the two incident beam momenta used in the experiment. The widths of the peaks correspond to the intrinsic momentum bite combined with the effects of the energy loss as the beam traverses the chamber before interacting, and the fitting error. Since the maximum

FIGURE 2-1

PROBABILITY DISTRIBUTION 3 AND 4 PRONGS

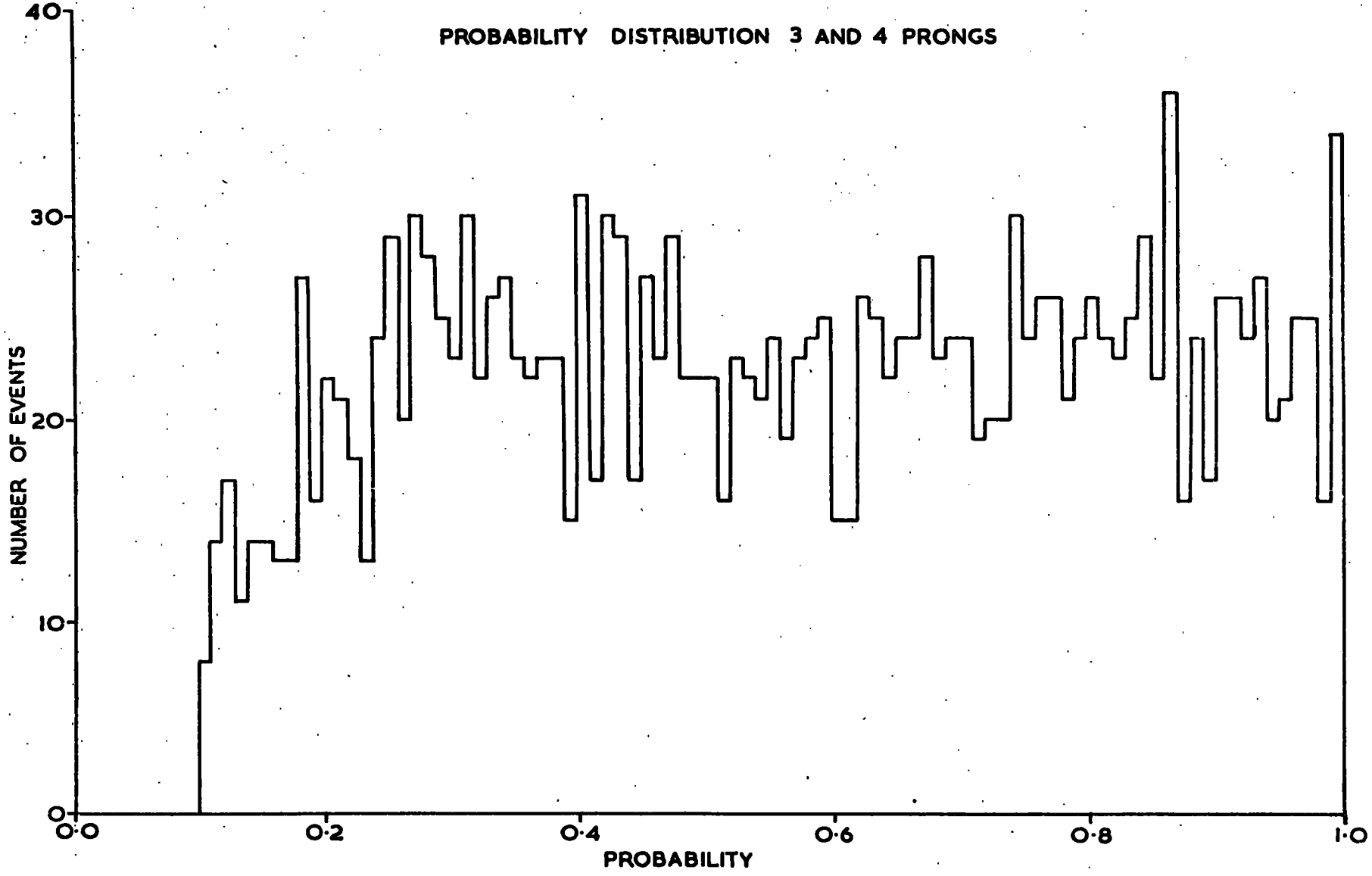

FIGURE 2-2

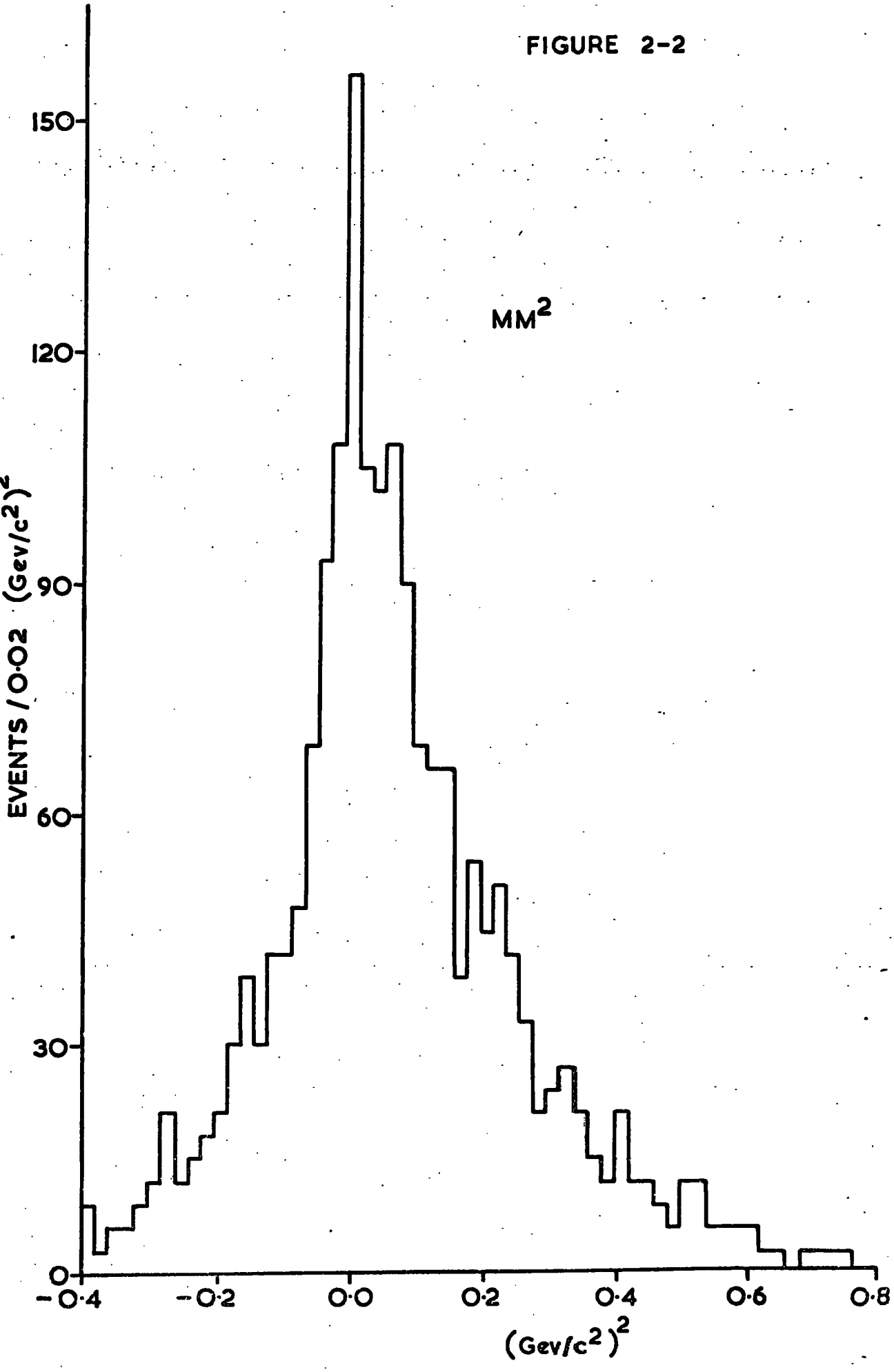
150
120
90
60
30
0
EVENTS / 0·02 (Gev/c²)²
MM²
-0·4
-0·2
0·0
0·2
0·4
0·6
0·8
(Gev/c²)²

FIGURE 2-3

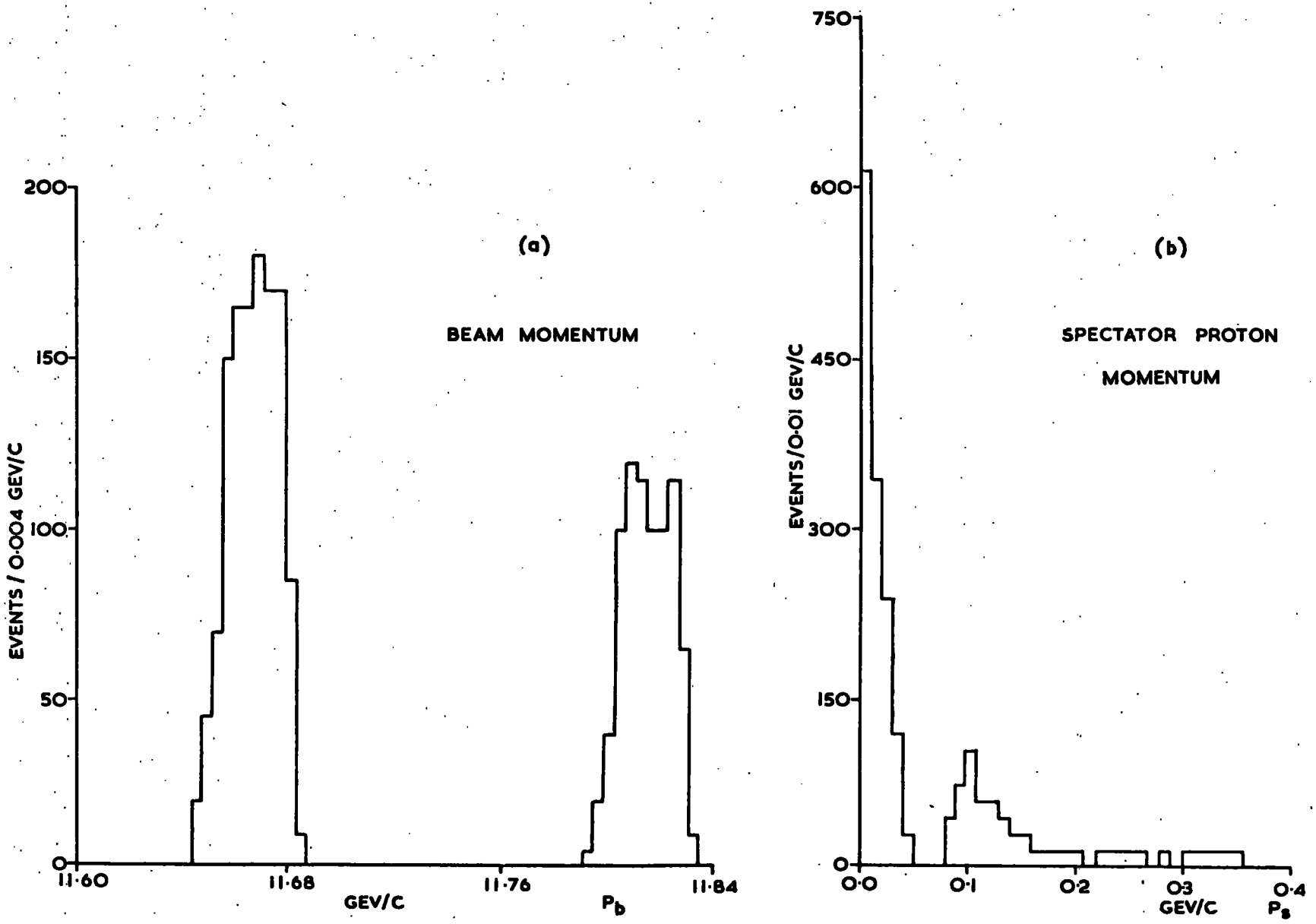
(a)
BEAM MOMENTUM
EVENTS / 0·004 GEV/C
200
150
100
50
0
11·60
11·68
11·76
11·84
GEV/C
P_b
(b)
SPECTATOR PROTON
MOMENTUM
EVENTS/0·01 GEV/C
750
600
450
300
150
0
0·0
0·1
0·2
0·3
0·4
GEV/C
P_s

FIGURE 2-3

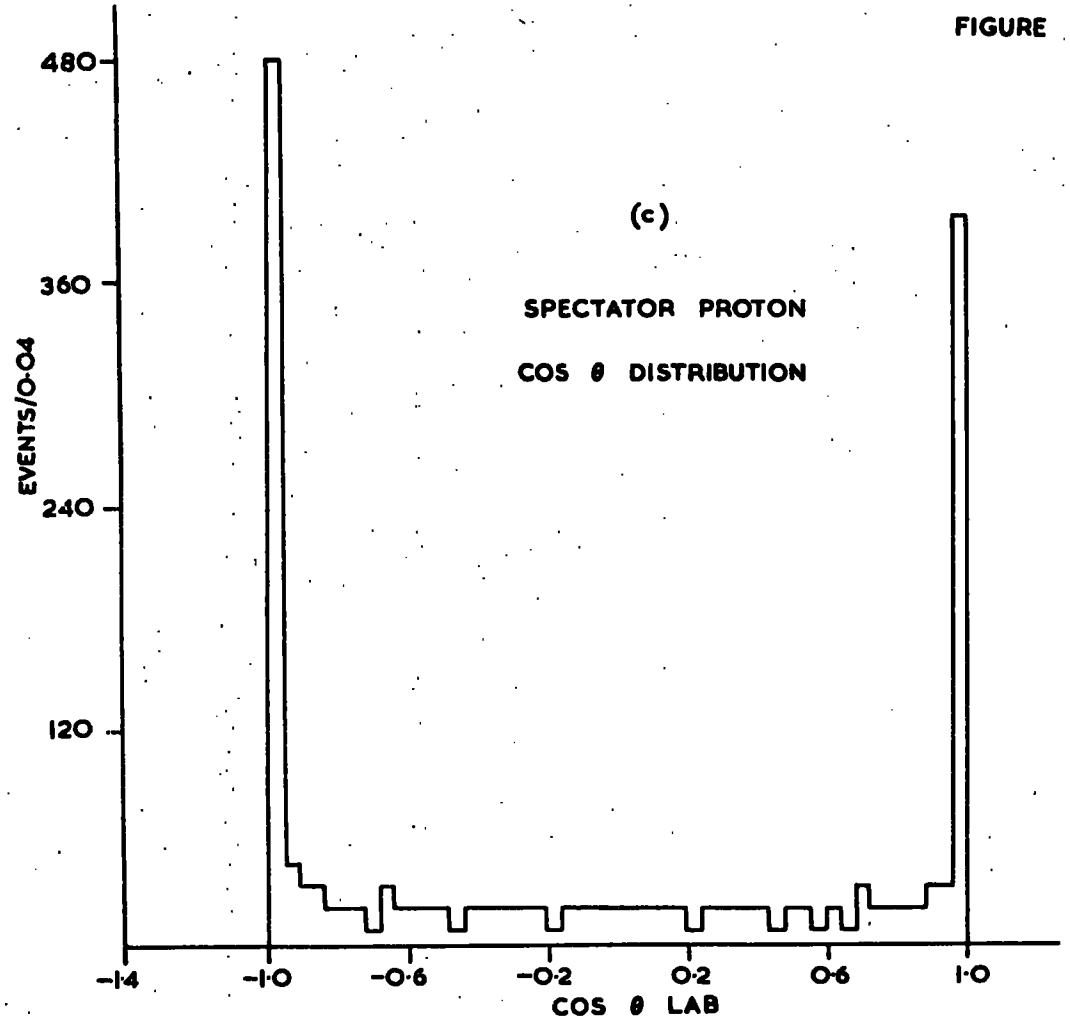
(c)
SPECTATOR PROTON
COS θ DISTRIBUTION
EVENTS/0·04
480
360
240
120
-1·4
-1·0
-0·6
-0·2
0·2
0·6
1·0
COS θ LAB

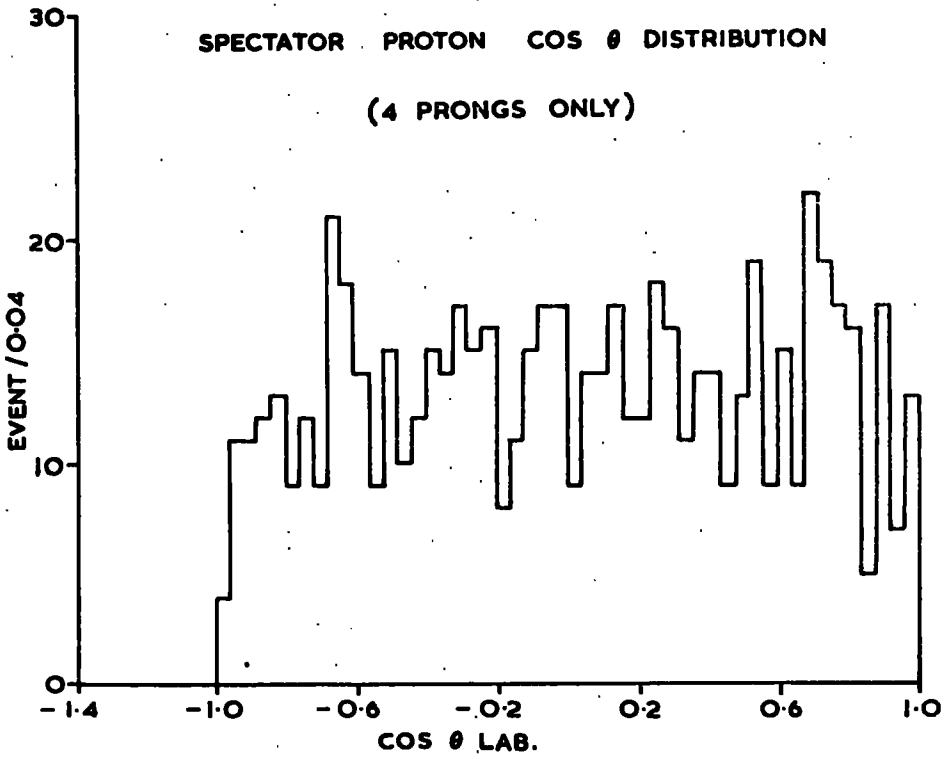
(d)
SPECTATOR PROTON COS θ DISTRIBUTION
(4 PRONGS ONLY)
EVENT / 0·04
30
20
10
0
-1·4
-1·0
-0·6
-0·2
0·2
0·6
1·0
COS θ LAB.

length of the beam track measured was about 100cm there can be a variation of about 25 MeV/c in the beam momenta used as starting values for GRIND. It is a reflection of the relatively small error given to this nominal beam momentum that the total width of each peak is only about 40 MeV/c.

The peak at low momentum values in the spectator momentum distribution Fig. 2-3(B) corresponds to the three prong events where the spectator is unseen. The events above 80 MeV/c are the four prong events where the spectator is seen and measured. Since even the four prong events in this channel are only one constraint fits, one would not expect the three prong events, which have two unseen particles (the spectator proton as well as the π^o, to reproduce the expected Hulthen momentum distribution for the spectator proton. This is also reflected in the angular distribution of the spectator proton with respect to the beam in the laboratory system, as shown in the same figure. The three prongs contribute mostly to the peaks near $\cos\theta = \pm 1$, while the four prong events display an isotropic distribution (Fig. 2-3(D). This isotropy would be expected for a spectator since it takes no part in the interaction and hence has no special reference direction. However, as Appendix (A) shows, the poor description of the spectator has comparatively little effect on the invariant masses

of the various baryon and meson systems.

In Fig 2-4 are shown the momenta and angular distributions of the outgoing pions and the fast proton. The angular distributions are again referred to the beam direction in the laboratory and in all cases the three prong and four prong distributions are comparable. The distributions show:-

(A) Almost all particles travel forwards in the laboratory system.

(B) The pions are more forward peaked than the proton, the π^+ being the most strongly peaked.

(C) The π^- and π^0 distributions are very similar with only a low momentum peak and a relatively flat distribution at high momenta. This is in contrast with the π^+ distribution which has a smaller low momentum peak and also shows a high momentum peak, suggesting that there are some 'leading' pions.

(D) The fast proton is of relatively low momentum. The distribution is still dropping at 1.2 GeV/c where the momentum selection was imposed.

2.2 Mass Distributions

Goldhaber plots are shown in Fig. 2-5 (A) and (B) for $M(p\pi^0)/M(\pi^+\pi^-)$ and $M(p\pi^-)/M(\pi^+\pi^0)$ respectively. Scatter plot (A) shows clear evidence for a ρ^0 band with perhaps an f^0 band as well. There

FIGURE 2-4

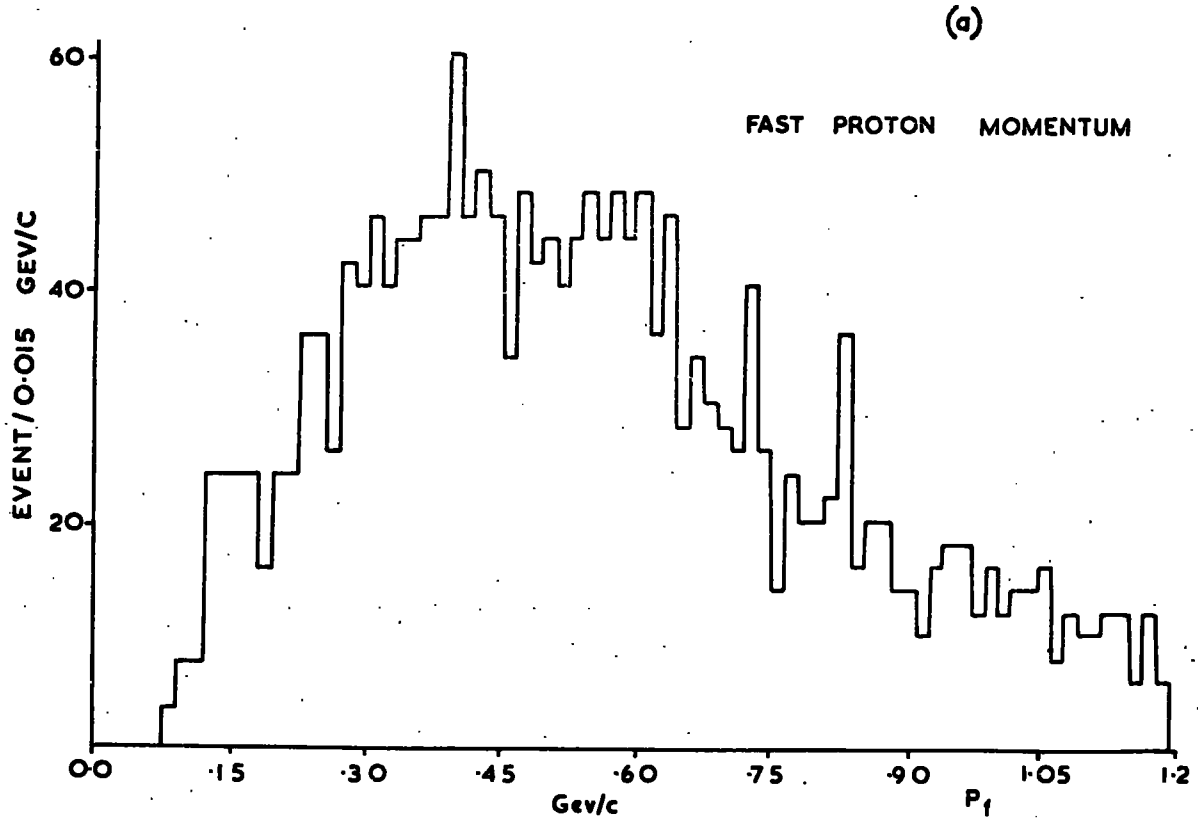
(a)
FAST PROTON MOMENTUM
EVENT/0·015 GEV/C
60
40
20
0·0
·15
·30
·45
·60
·75
·90
1·05
1·2
Gev/c
P_f

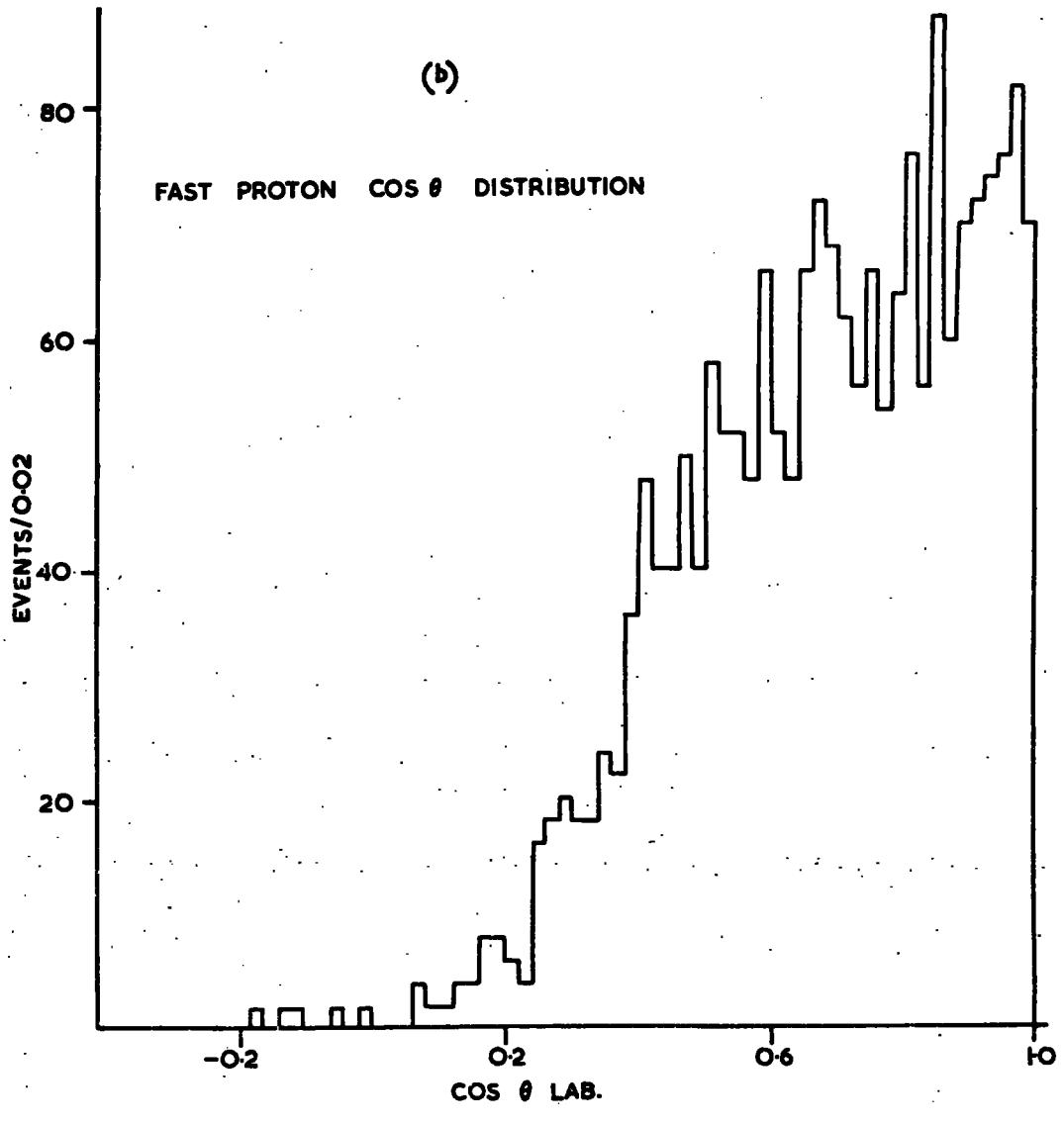
(b)
FAST PROTON COS θ DISTRIBUTION
EVENTS/0·02
80
60
40
20
-0·2
0·2
0·6
1·0
COS θ LAB.

FIGURE 2-4

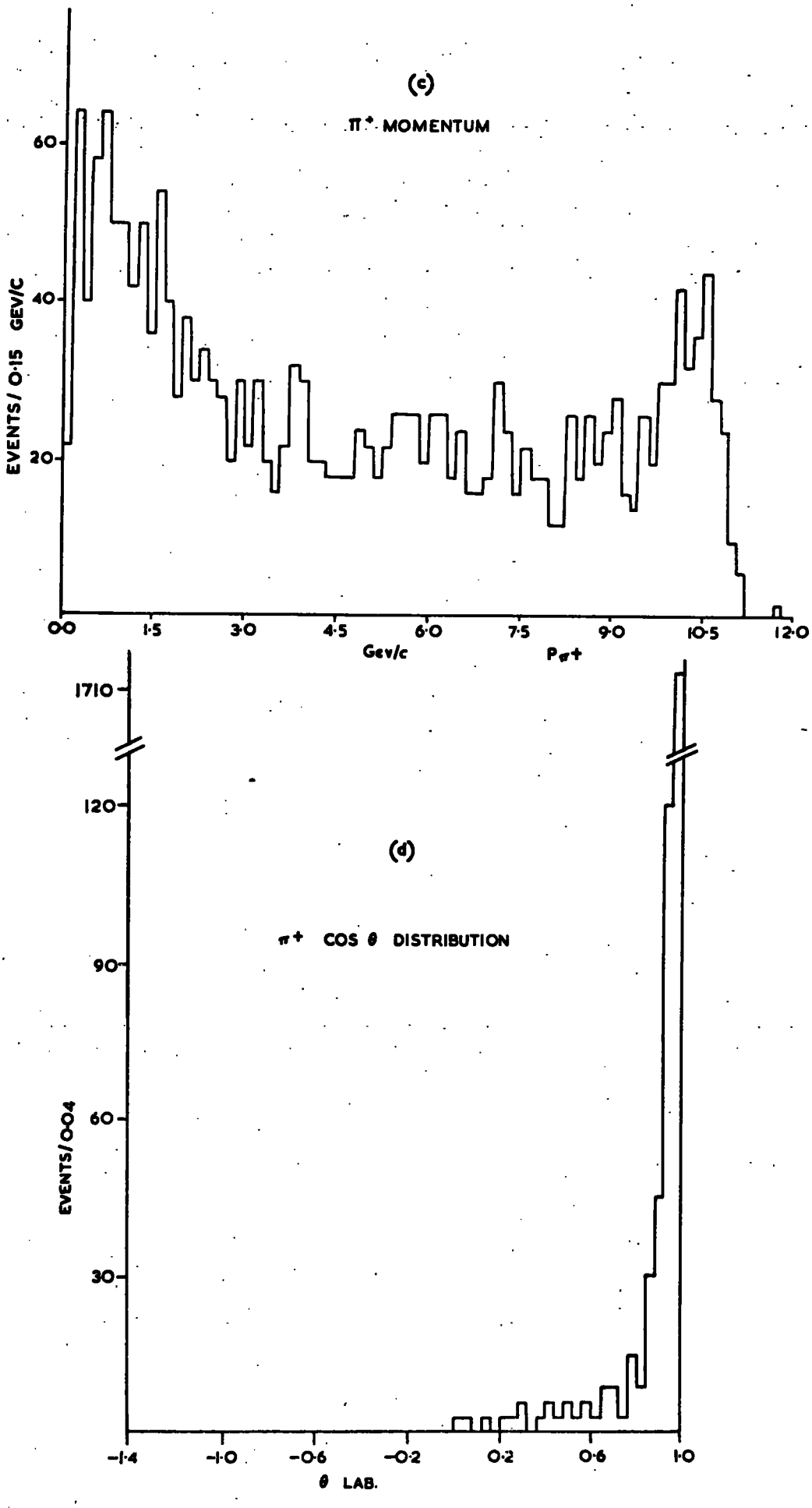
(c)
π+ MOMENTUM
EVENTS/ 0·15 GEV/C
60
40
20
0·0
1·5
3·0
4·5
6·0
7·5
9·0
10·5
12·0
Gev/c
Pπ+
(d)
π+ COS θ DISTRIBUTION
EVENTS/0·04
1710
120
90
60
30
-1·4
-1·0
-0·6
-0·2
0·2
0·6
1·0
θ LAB.

FIGURE 2-4

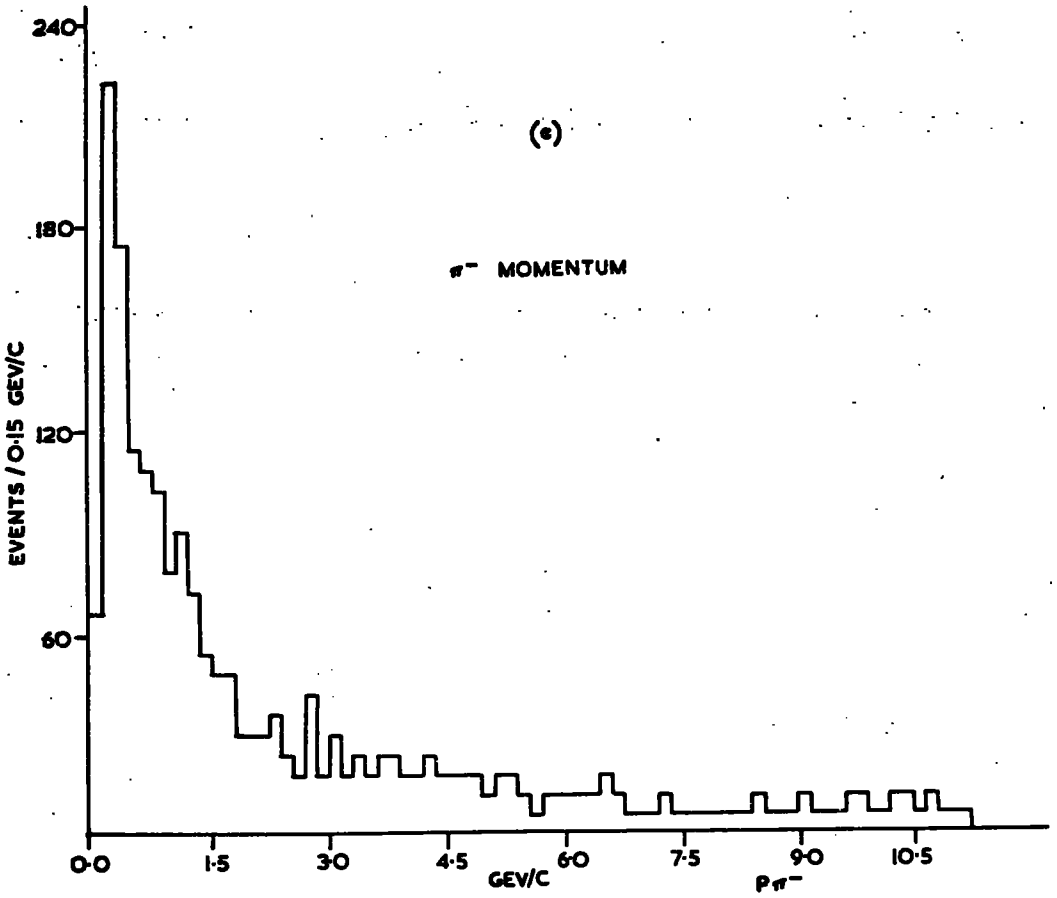
(e)
π^- MOMENTUM
EVENTS / 0·15 GEV/C
240
180
120
60
0·0
1·5
3·0
4·5
6·0
7·5
9·0
10·5
GEV/C
P_{π^-}

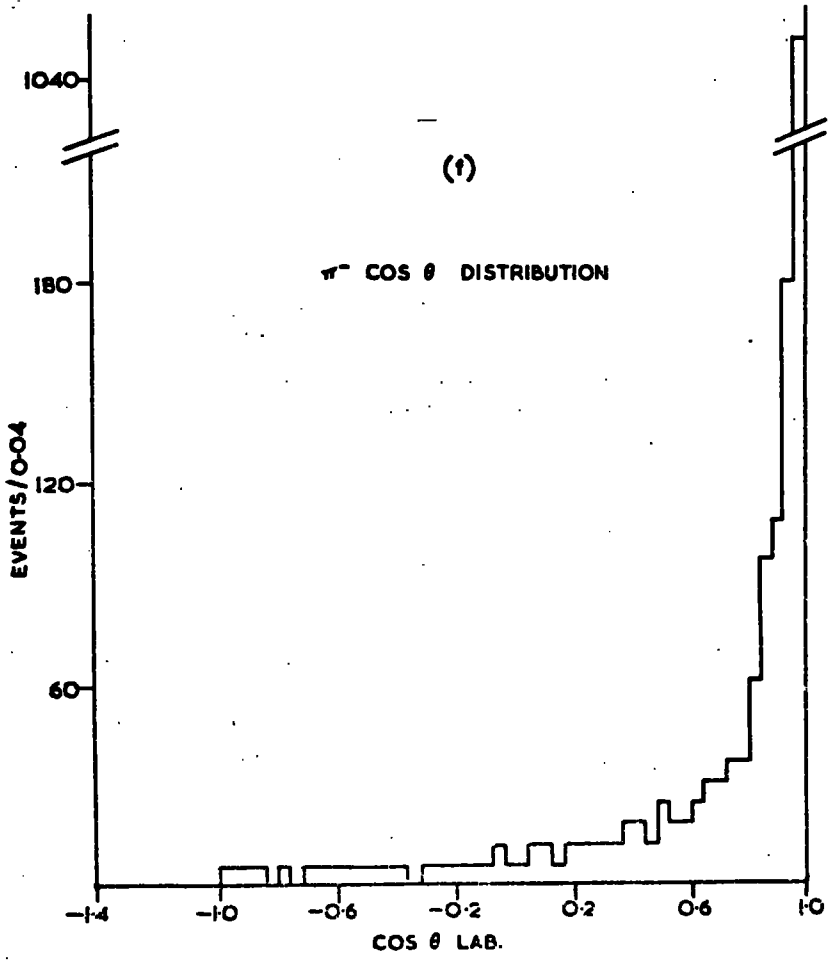
(f)
π^- COS θ DISTRIBUTION
EVENTS / 0·04
1040
180
120
60
−1·4
−1·0
−0·6
−0·2
0·2
0·6
1·0
COS θ LAB.

FIGURE 2-4

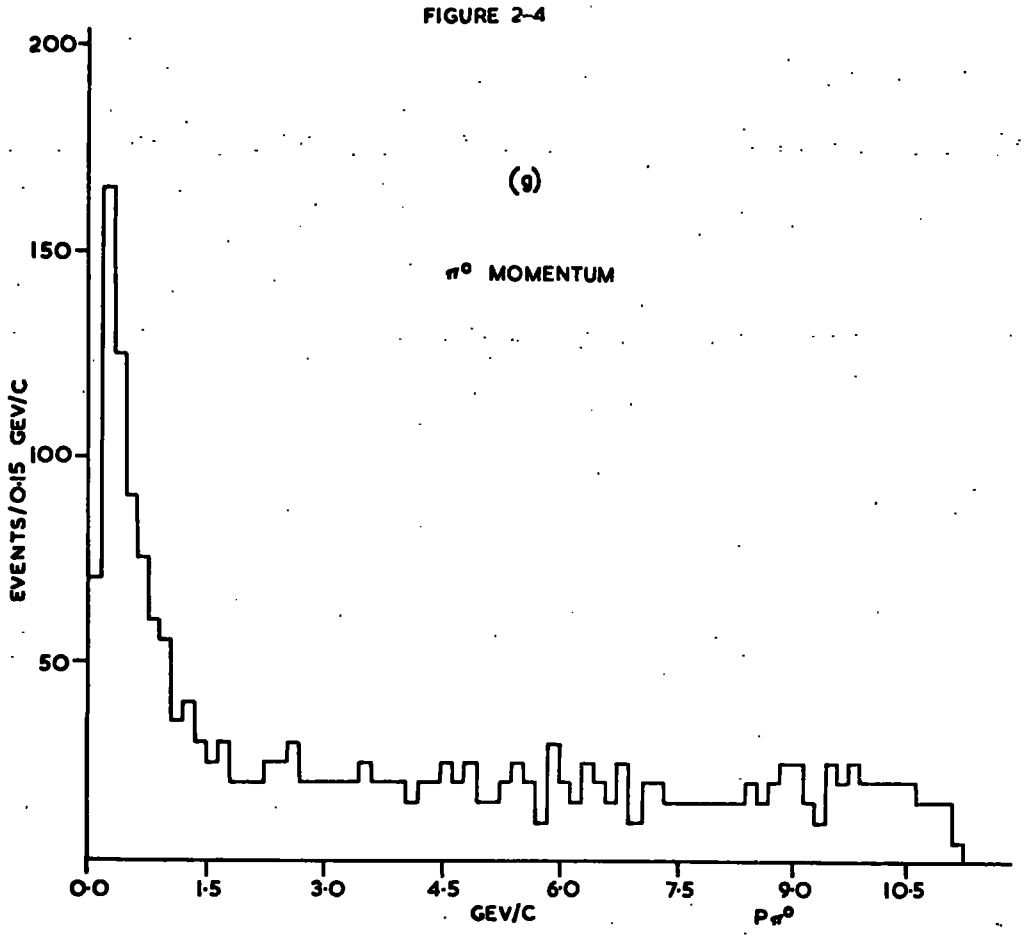
(g)
π^0 MOMENTUM
EVENTS/0·15 GEV/C
200
150
100
50
0·0
1·5
3·0
4·5
6·0
7·5
9·0
10·5
GEV/C
P_{π^0}

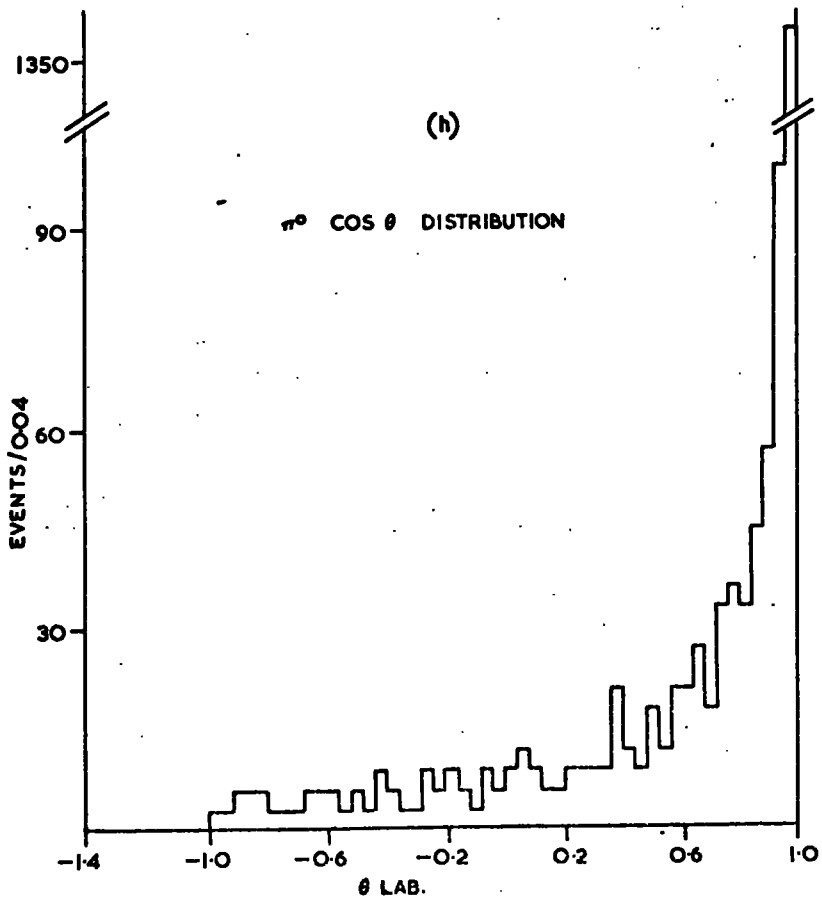
(h)
π^0 COS θ DISTRIBUTION
EVENTS/0·04
1350
90
60
30
−1·4
−1·0
−0·6
−0·2
0·2
0·6
1·0
θ LAB.

FIGURE 2-5

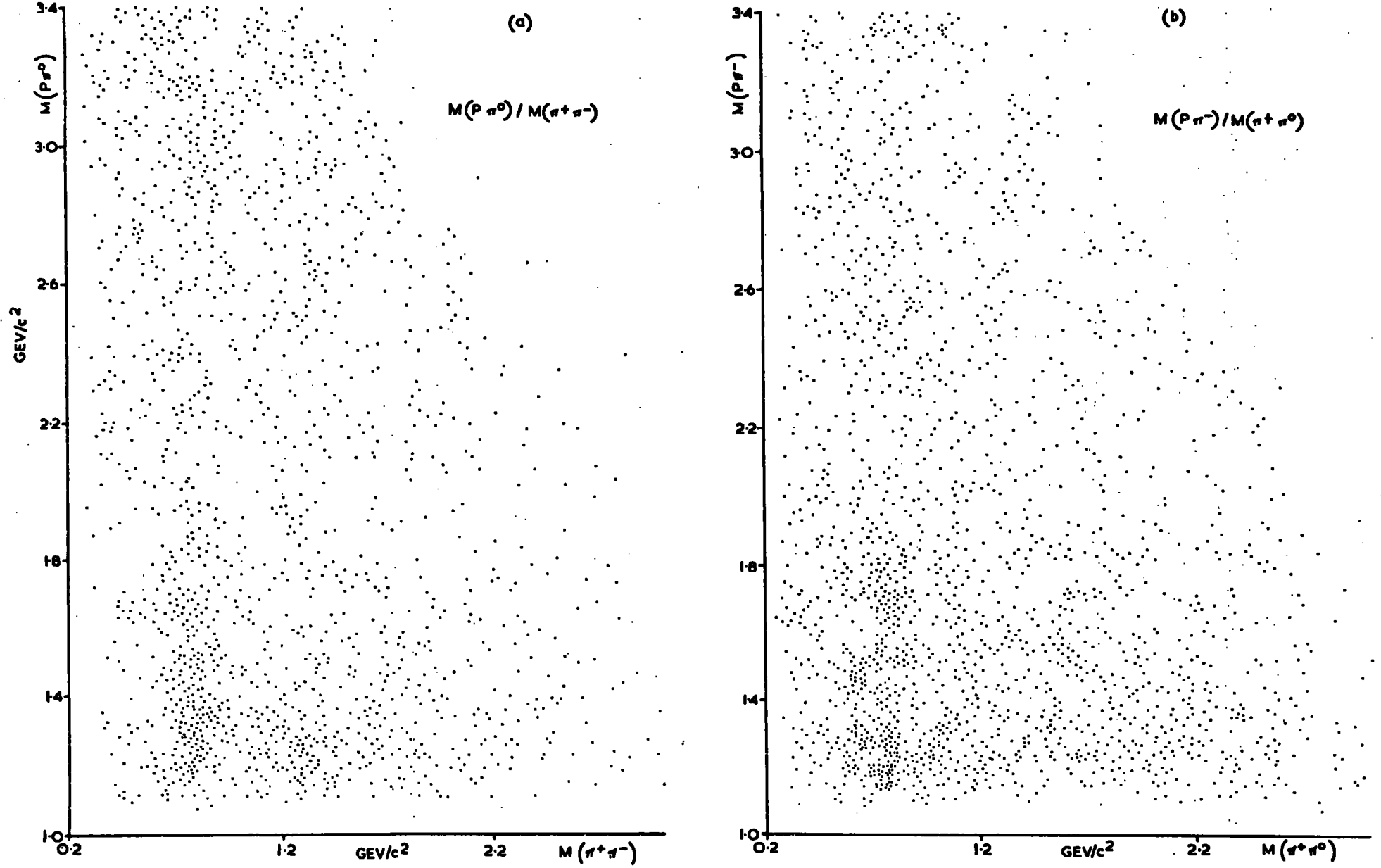
(a)
M(P π⁰) / M(π⁺π⁻)
M(P π⁰)
GEV/c²
3·4
3·0
2·6
2·2
1·8
1·4
1·0
0·2
1·2
2·2
M (π⁺π⁻)
(b)
M(P π⁻) / M(π⁺π⁰)
M(P π⁻)
GEV/c²
M (π⁺π⁰)

is also a possible N^{*+} band although much of the signal is from the ρ^0 and f^0 overlap regions. On scatter plot (B) the only clear band corresponds to the ρ^+ although there is also the possibility of an N^{*0} band. On both Goldhaber plots there is some evidence for N^* resonances other than the $N^*(1236)$ (or the $\Delta(1236)$), and possibly $\Delta\rho$ and $\Delta^+ f^0$ associated production.

The projections of these plots are shown on Figs. 2-6 and 2-7 respectively and in each case the dipion spectrum is also shown for the four prong events only.

The $M(\rho\pi^0)$ mass distribution shows evidence for considerable $\Delta^+(1236)$ production. However, the possibly large and rapidly varying background in this region makes mass and width determination very difficult. This also makes any interpretation of the possible enhancements at 1440 and 1580 MeV/c^2 impossible.

The $M(\pi^+\pi^-)$ mass distributions are also shown on Fig.2-6(B) and (C). A clear ρ^0 signal can be seen despite considerable background. The signal to background ratio is considerably better in the four prong distribution than it is in the combined three and four prong distribution. Although there is evidence for enhancement in the region of the $f^0(1260)$ the poor shape of the distribution and the relatively low statistics involved make any determination of mass and width meaningless. Similarly, the small enhancement in the g^0 mass region has little statistical

FIGURE 2-6

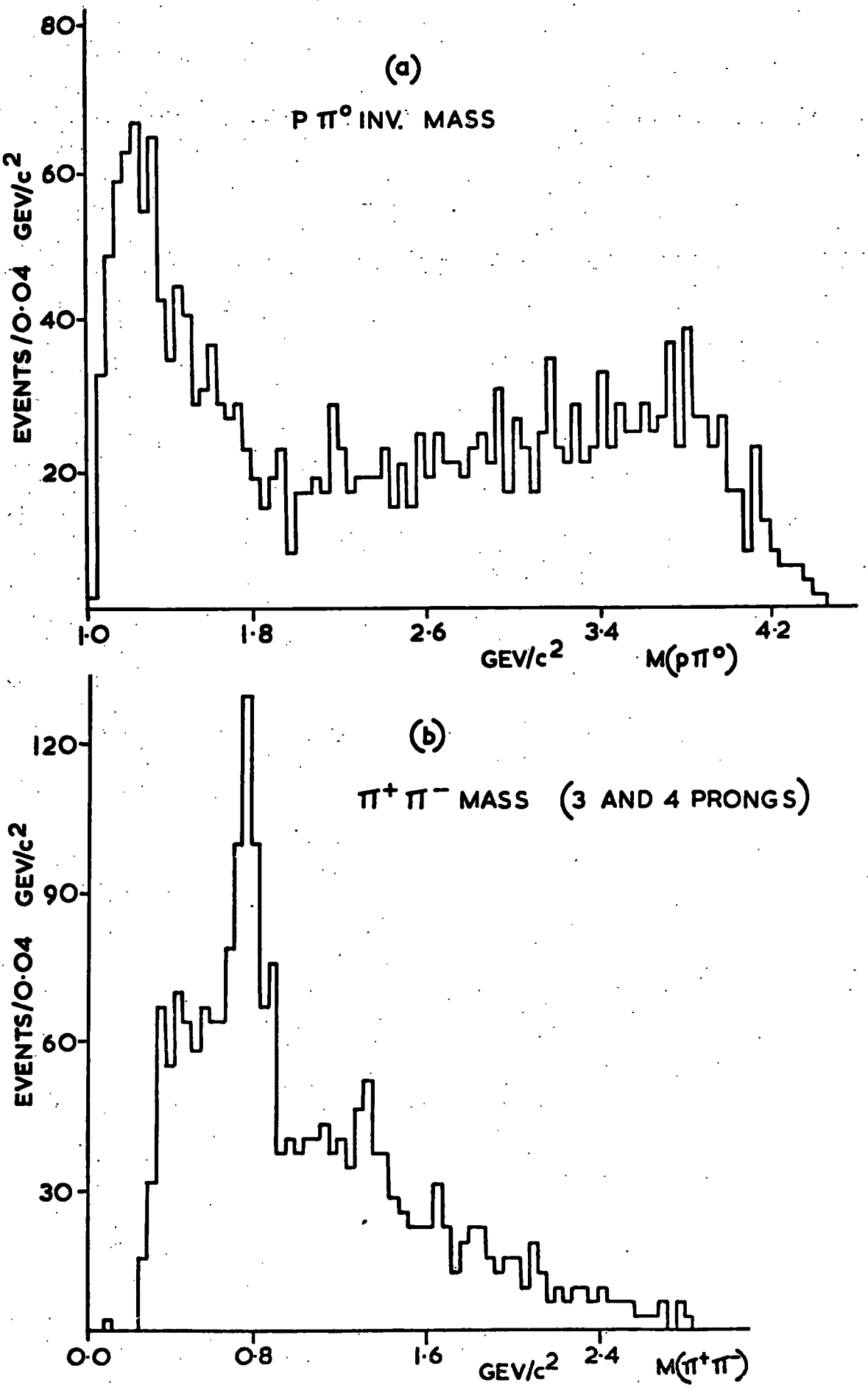
(a)
P π° INV. MASS
EVENTS/0·04 GEV/c²
80
60
40
20
1·0
1·8
2·6
3·4
4·2
GEV/c²
M(pπ°)
(b)
π⁺π⁻ MASS (3 AND 4 PRONGS)
EVENTS/0·04 GEV/c²
120
90
60
30
0·0
0·8
1·6
2·4
GEV/c²
M(π⁺π⁻)

FIGURE 2-6

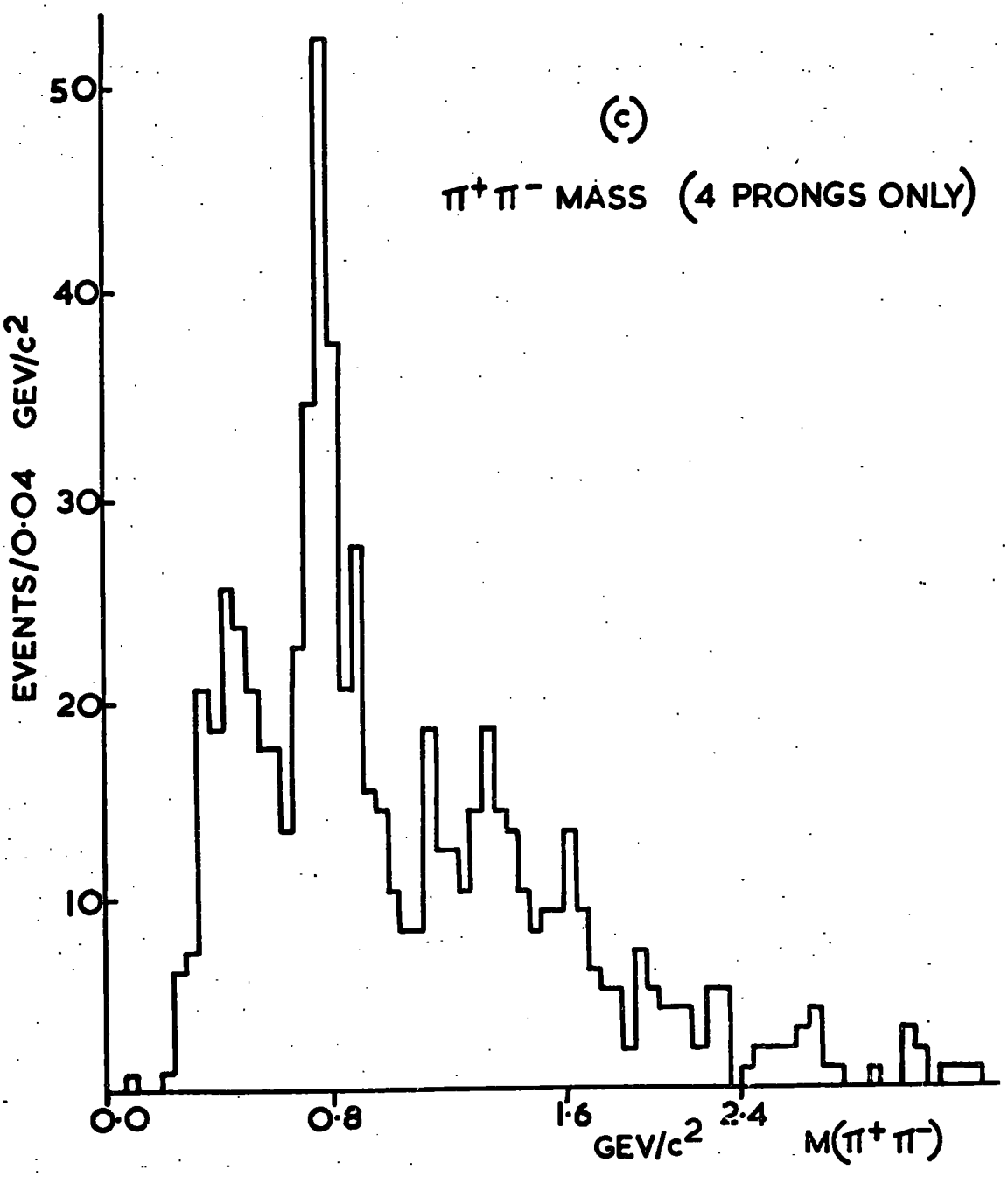
(c)
$\pi^+\pi^-$ MASS (4 PRONGS ONLY)
EVENTS/0·04 GEV/c²
50
40
30
20
10
0·0
0·8
1·6
2·4
GEV/c²
M($\pi^+\pi^-$)

significance. Later it will be shown that the accumulation in the dipion spectrum below the ρ^0 mass is due in part to ω^0 production.

The $M(p\pi^-)$ and $M(\pi^+\pi^0)$ mass distributions are shown in Fig. 2-7(A), (B) and (C). The $\Delta(1236)$ has a better defined shape in the $M(p\pi^-)$ than it has in the $M(p\pi^0)$ mass distribution. One reason for this is that the unseen (and therefore unmeasured) π^0 is used in the $M(p\pi^0)$ while the $M(p\pi^-)$ uses two measured tracks, thus having a better mass resolution. Another reason is perhaps that there are more Δ^0 events than there are Δ^+ events, as would be expected from Clebsch-Gordan coefficients.

There is also evidence for higher mass N^* resonances at about 1480 MeV/c^2 and 1680 MeV/c^2 although no real significance can be given to these due to the uncertain background.

The $M(\pi^+\pi^0)$ mass distribution shows a ρ^+ peak, the shape of which is considerably improved when only four prong events are considered. No other significant enhancements can be seen.

The $M(\pi^+\pi^-\pi^0)$ and the $M(\pi^-\pi^0)$ mass distributions are shown in Fig. 2-8 (A), (B) and (C). The only obvious tripion enhancement corresponds to the ω^0 mass although there is a small enhancement in the η^0 mass region. There is no evidence for A_2^0 production or for any other resonance production in either the

FIGURE 2-7

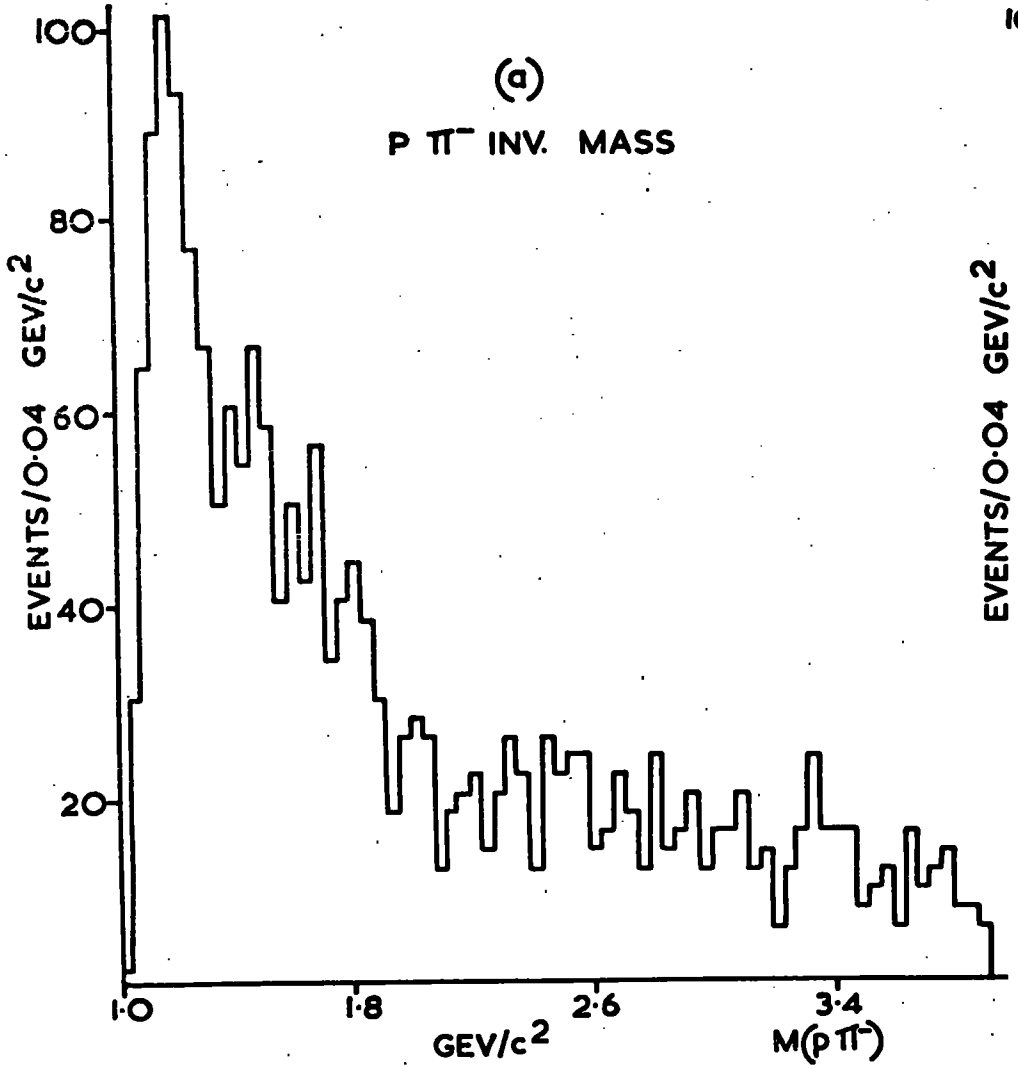
(a)
P π⁻ INV. MASS
EVENTS/0·04 GEV/c²
100
80
60
40
20
1·0
1·8
2·6
3·4
GEV/c²
M(p π⁻)

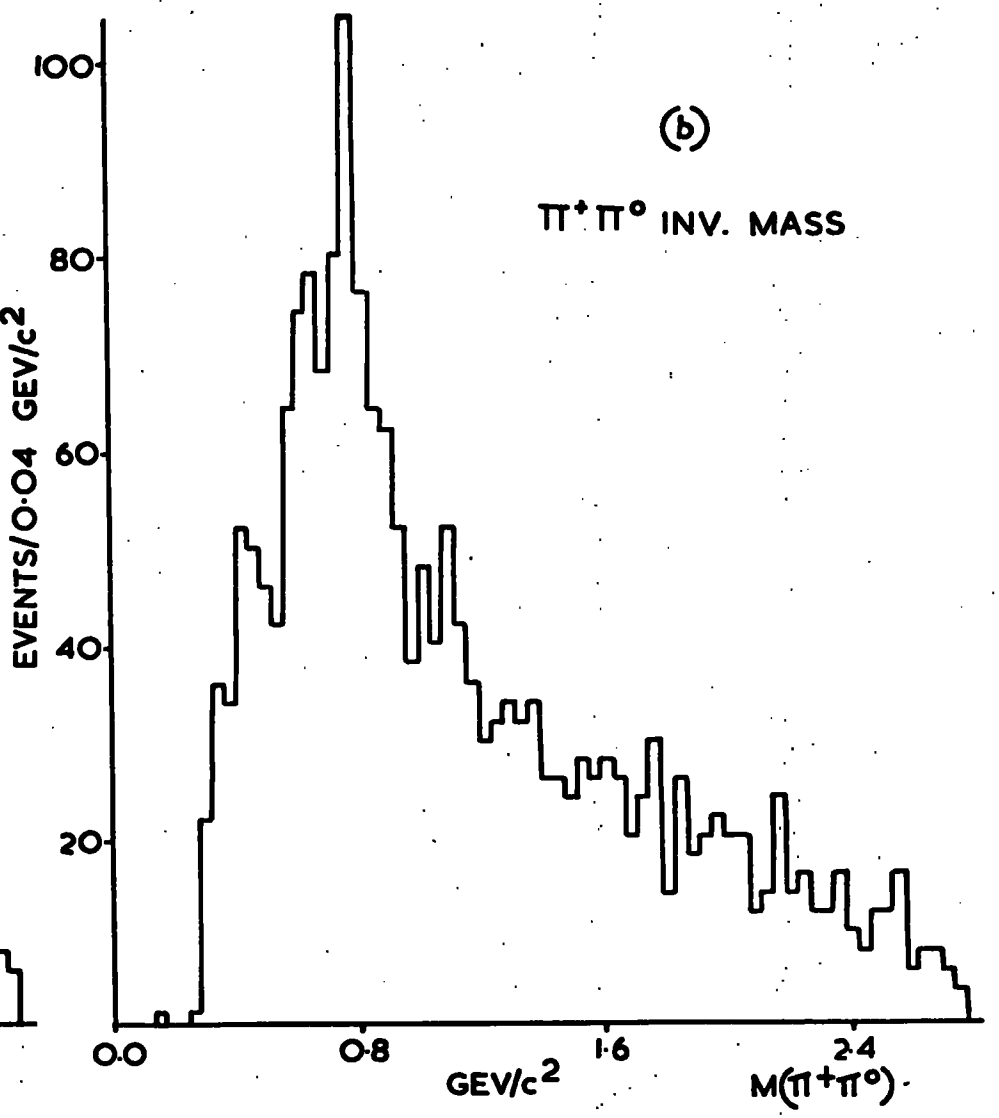
(b)
π⁺π° INV. MASS
EVENTS/0·04 GEV/c²
100
80
60
40
20
0·0
0·8
1·6
2·4
GEV/c²
M(π⁺π°)

FIGURE 2-7

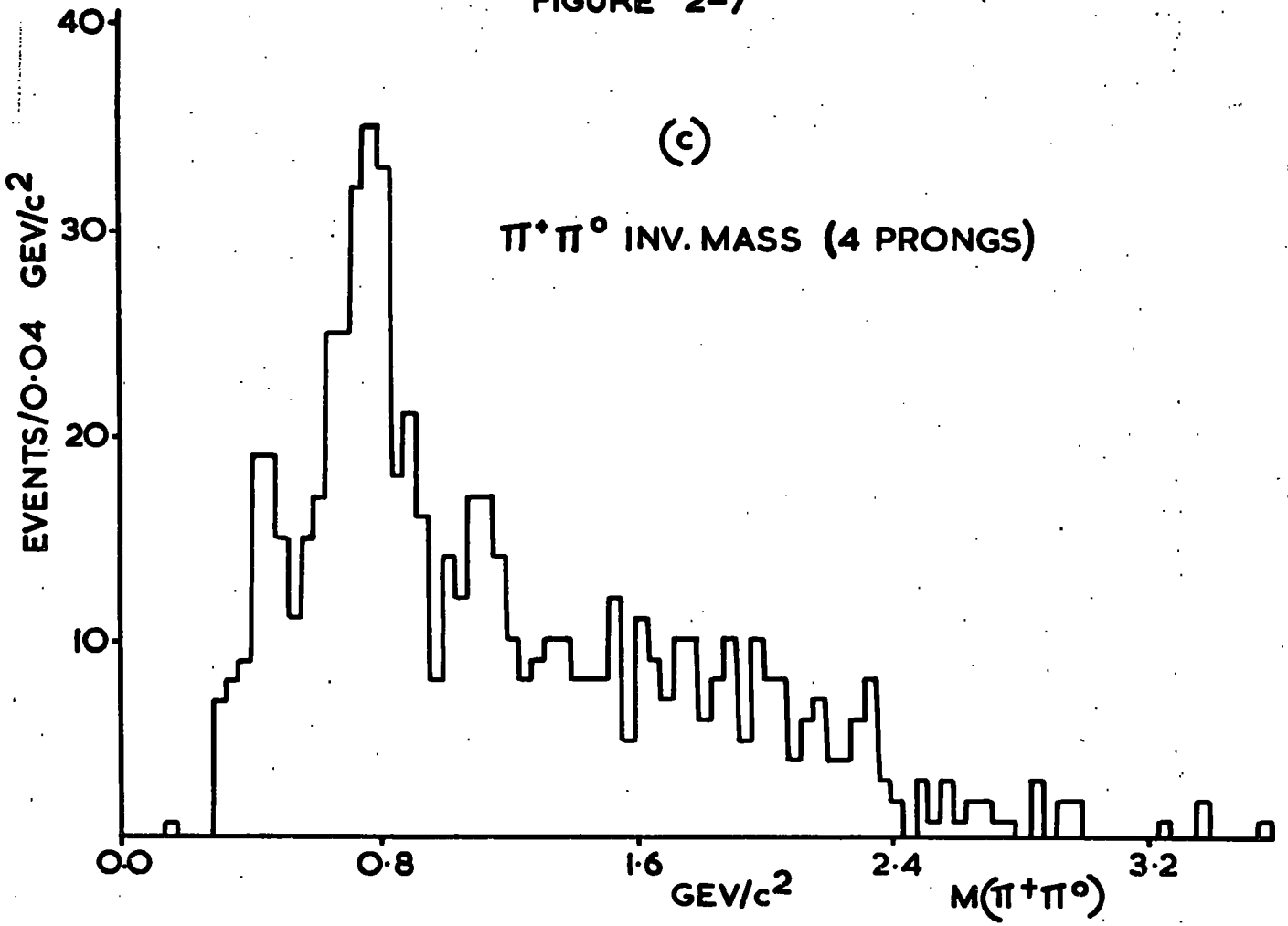
(c)
$\pi^+\pi^0$ INV. MASS (4 PRONGS)
EVENTS/0·04 GEV/c²
40
30
20
10
0·0
0·8
1·6
2·4
3·2
GEV/c²
M(π⁺π⁰)

FIGURE 2-8

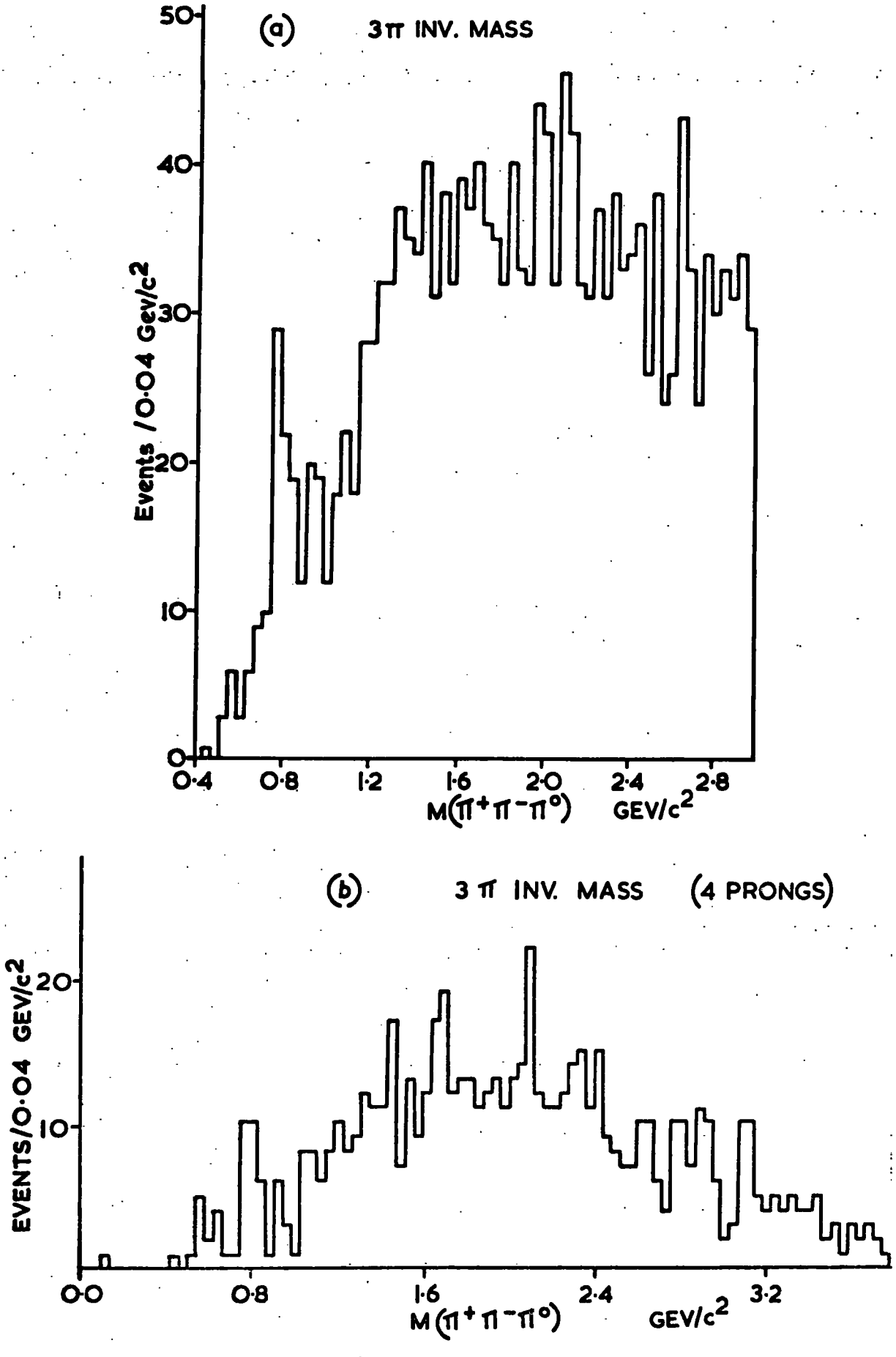
(a) 3π INV. MASS
Events /0·04 Gev/c²
50
40
30
20
10
0
0·4
0·8
1·2
1·6
2·0
2·4
2·8
M(π⁺π⁻π°) GEV/c²
(b) 3 π INV. MASS (4 PRONGS)
EVENTS/0·04 GEV/c²
20
10
0·0
0·8
1·6
2·4
3·2
M(π⁺π⁻π°) GEV/c²

FIGURE 2-8

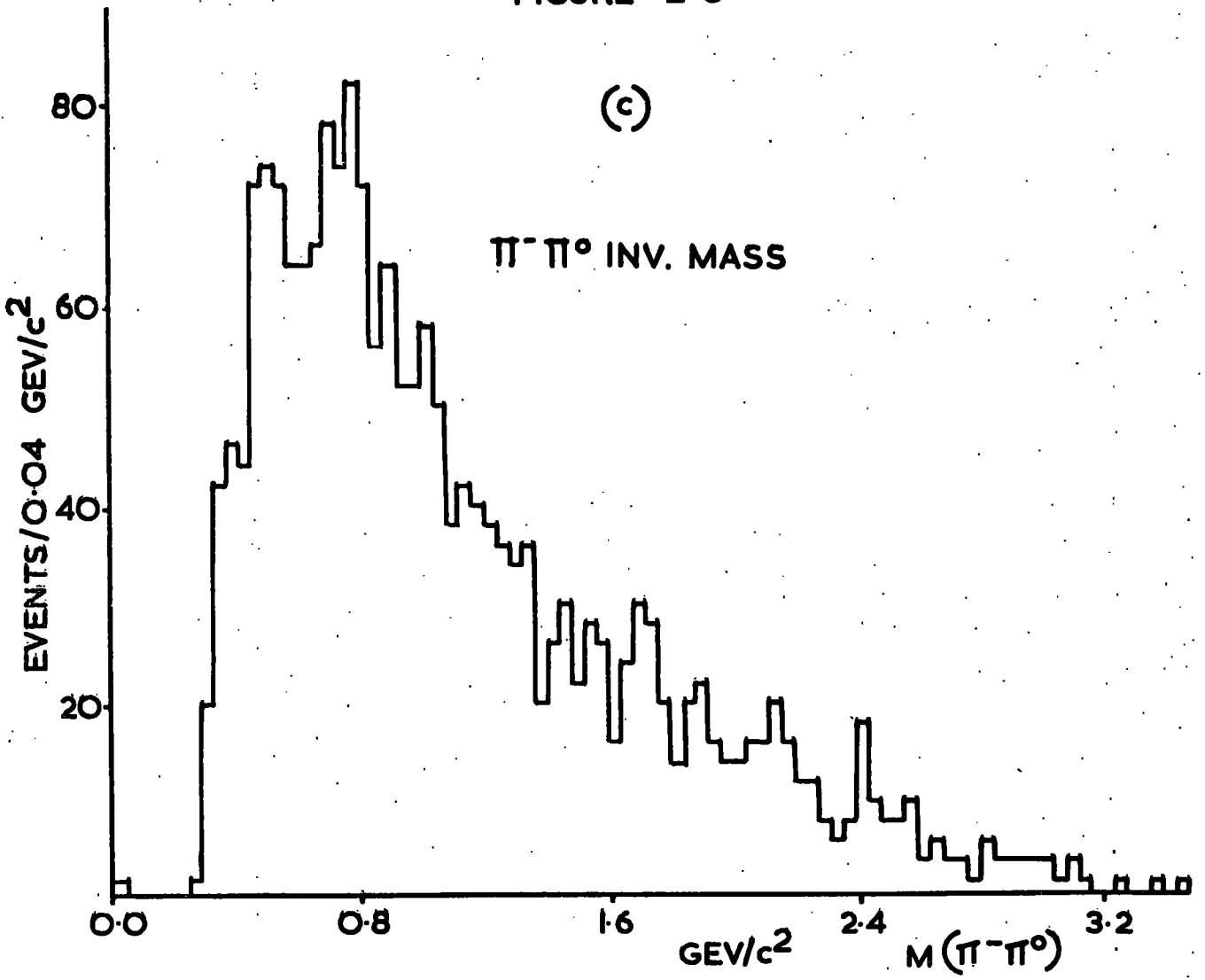
(c)
π⁻π° INV. MASS
EVENTS/0·04 GEV/c²
80
60
40
20
0·0
0·8
1·6
2·4
3·2
GEV/c²
M(π⁻π°)

total tripion mass distribution (which has a higher background) or in the four prong only mass distribution (which has poor statistics), although there is a possibility of H(900) production.

The $M(\pi^- \pi^0)$ mass distribution only shows the possibility of a small amount of ρ^- production on a very high background level.

There are no enhancements or significant resonance shapes in the $M(\rho \pi^+)$ mass spectrum.

From these distributions it can be seen that in order to make full use of the moderate statistics available it is preferable to attempt to use the three prong events wherever possible.

CHAPTER 3

THE VAN HOVE (L.P.S.) METHOD OF ANALYSIS

3.1 Introduction

The very important technique of Longitudinal Phase Space (L.P.S.) analysis was suggested by Van Hove (Ref.5). It is found experimentally that most events are peripheral in nature, that is, in the centre of mass (or more correctly, in the centre of momentum system) the longitudinal component of the momentum is, in general, much larger than the transverse component. Typically, experimental data show that while the longitudinal component of momentum varies between zero and the kinematically allowed limit, the transverse component displays a marked lack of events with momentum values above about 0.4 GeV/c. This led Van Hove to suggest that events could be adequately parameterised by the longitudinal component of momentum alone.

Considering the Feynman diagram, which is a two dimensional plot of the separation between the interacting particles in the centre of mass against time, Van Hove's parameterisation means that in general a positive longitudinal momentum (q) can be associated with the upper vertex (the beam vertex, by convention), while a negative q can be associated with the lower (baryon) vertex.

The possible (simple) Feyman diagrams for the reaction are:-

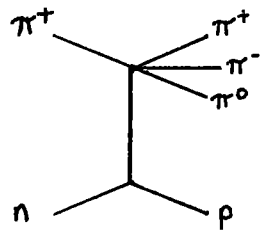

1

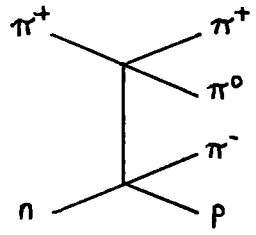

2

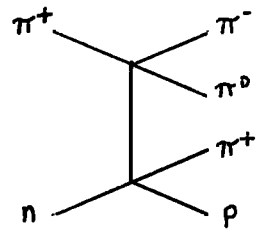

3*

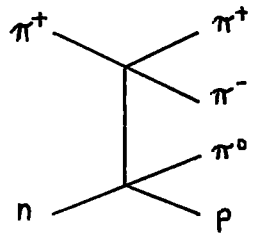

4

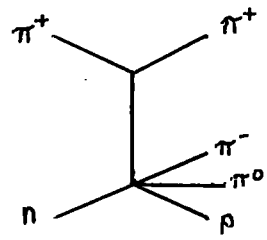

5

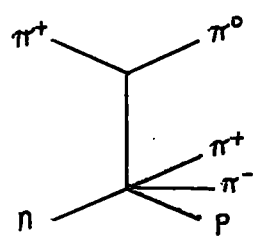

6

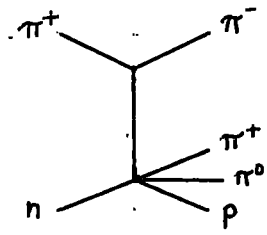

7*

* Exotic

If the particles are to form a low mass resonance, they must have low relative momenta in the centre of

mass frame and so must also have similar values of q. This implies that particular low mass resonances will populate certain regions of longitudinal phase space, suggesting a simple method of sub-dividing data into various groups which will then be rich in particular resonances. A four body final state has been discussed by Van Hove and others in terms of L.P.S (Ref.5,6.)

The reason for the previous statement that this type of analysis is only useful for low mass resonances is simply explained. If a resonance has a mass value which is well above threshold for the system considered, then a large amount of energy will be released as kinetic energy when the resonance decays. This implies that at least one decay product might travel in the opposite direction to the other decay products when viewed in the overall centre of mass system, provided the resonance mass was high enough to provide the necessary energy. Of course, even a low mass resonance can be affected by this if the system is produced with a small longitudinal component of momentum originally. However, a small longitudinal momentum for a low mass system would normally suggest a high transverse momentum component and, since most interactions are peripheral in nature, low mass systems would display this effect much less frequently than higher mass systems.

3.2. Definition of Variables

Although there are four parameters to describe an event (the four q.s), these will produce a unique point in a three dimensional space because of the conservation of longitudinal momentum. In the centre of mass system, and using appropriate axes, all events will lie inside a cuboctahedron, the faces of which will correspond to various combinations of particles travelling in the same direction in the centre of mass. The cuboctahedron can be described using a spherical polar co-ordinate system based on the centre of the cuboctahedron. In a Cartesian (X,Y,Z) system, the four q=0 axes are chosen to be mutually separated by 120 degrees. The spherical polar system ($R, \vartheta_1, \vartheta_2$) can then be defined. Fig. 3-1 shows the cuboctahedron and also the equations which relate the various co-ordinate systems (Ref. 6, 7).

The ϑ_1, ϑ_2 parameters define which face on the surface of the cuboctahedron the projected radius vector ($\vec{r}$) will intersect. If the projection intersects a square face, it implies that only two particles have positive values of q, whereas intersection on a triangular face implies that three particles have values of q with the same sign.

The length of the radius vector ($\vec{r}$) of a point in the L.P.S. cuboctahedron is related to the peripherality of an event corresponding to that point

FIGURE 3-1

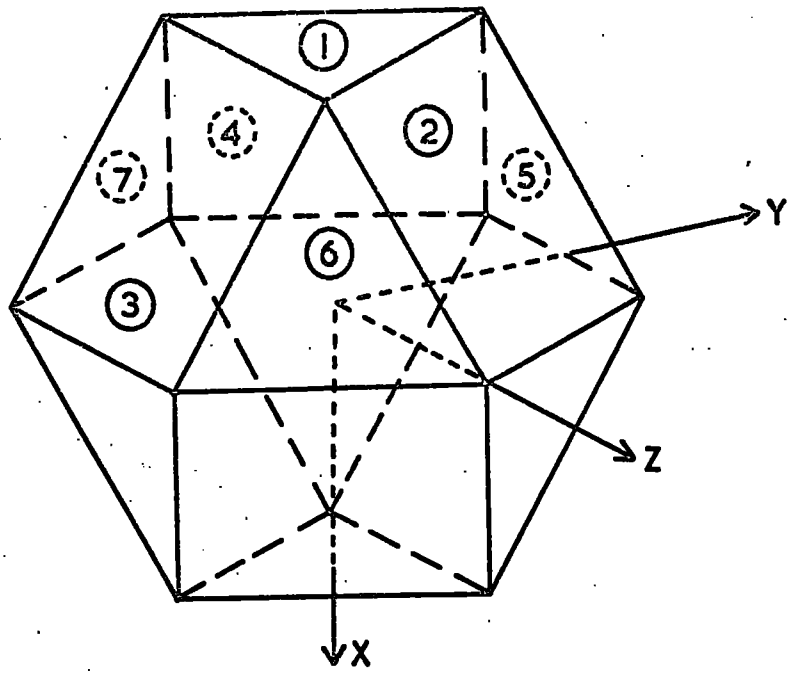

LPS CUBOCTAHEDRON

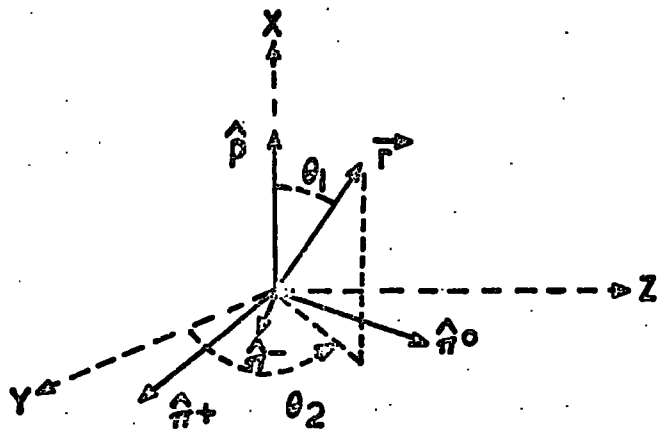

$\hat{p} = (1,0,0)$

$\hat{\pi}^+ = \left(-\frac{1}{3}, \frac{2\sqrt{2}}{3}, 0\right)$

$\hat{\pi}^- = \left(-\frac{1}{3}, -\frac{\sqrt{2}}{3}, -\frac{\sqrt{6}}{3}\right)$

$\hat{\pi}^0 = \left(-\frac{1}{3}, -\frac{\sqrt{2}}{3}, \frac{\sqrt{6}}{3}\right)$

$q_p = \hat{p} \cdot \vec{r}$

$q_{\pi^+} = \hat{\pi}^+ \cdot \vec{r}$

$q_{\pi^-} = \hat{\pi}^- \cdot \vec{r}$

$q_{\pi^0} = \hat{\pi}^0 \cdot \vec{r}$

$$r = \sqrt{\frac{3}{4}\left(q_p^2 + q_{\pi^+}^2 + q_{\pi^-}^2 + q_{\pi^0}^2\right)}$$

$$\theta_1 = \cos^{-1}\left(\frac{q_p}{r}\right)$$

$$\theta_2 = \tan^{-1}\left(\frac{\sqrt{3}\left(q_{\pi^0} - q_{\pi^-}\right)}{3q_{\pi^+} + q_p}\right)$$

but also depends on the conservation of energy and momentum. This means that even though an event may have a configuration which implies a maximum value of ($\vec{r}$), this value may not correspond to a point on the surface of the cuboctahedron. See Ref.5 for an account of this effect.

However, even with a three dimensional system, visualisation, analysis and presentation is still very difficult. A two dimensional system is preferable even if some of the available information is not displayed. This can be achieved in this case if the radius (R) is neglected. The data can then be usefully displayed by, for example, the use of a ϑ_1 , ϑ_2 scatter plot.

3.3. Definition of the centre of mass system

In order to calculate the values of the longitudinal momenta needed above, the centre of mass frame must first be defined. This is a problem because the interaction being studied, $\pi^+ n$, involves the neutron contained in a deuteron nucleus. This means that the momentum and effective mass of the target are unknown at the time of interaction, although the momentum distribution of the neutron is known from calculations based on the Hulthen distribution. There are several ways to approach this problem. Initially one can assume a target having the neutron's

mass but with zero momentum in the laboratory system. This gives a very rough approximation but it may be sufficient for some work. A second method involves assigning to the target neutron momentum equal and opposite to that of the spectator, since one can assume that the neutron and proton had equal and opposite momenta inside the deuteron at the moment of interaction. A refinement of this method is to constrain the $(n p_s)$ system to have the deuteron mass by allowing the neutron mass to be "off the mass shell", i.e. not to have its normal mass value. This generated target is then combined with the beam to produce the centre of mass system.

A third method is to combine the outgoing "reacting" particles to form the "reaction" centre of mass system. In this channel this corresponds to using the fast proton plus the three outgoing pions to define the centre of mass system. However, it can be seen that since the fitting in GRIND consists of conserving energy and momentum, i.e.:-

$$E_b + M_d c^2 = E_{p_s} + E_{p_f} + E_{\pi^+} + E_{\pi^-} + E_{\pi^0}$$

$$\vec{p}_b = \vec{p}_{p_s} + \vec{p}_{p_f} + \vec{p}_{\pi^+} + \vec{p}_{\pi^-} + \vec{p}_{\pi^0}$$

Where the subscript b corresponds to the beam and the P.s are three vectors of momentum, the second and third methods are identical. Since the third

method is easier to calculate, it was used to define the centre of mass system for all calculations.

The third method would appear to have an advantage over the second for three prong events where the spectator is unseen. However, for a 1C channel where a π^0 is also unseen, the available energy and momentum are shared between the spectator and the π^0 in a relatively arbitrary fashion. Since it would be pointless using anything other than the fitted spectator, especially for the three prong events, the second and third methods are again identical.

CHAPTER 4

THE RESULTS OF L.P.S. ANALYSIS

The Van Hove method of analysis relies on the experimental fact that the transverse component of momentum (r_i) of particles in the centre of mass is generally smaller than the longitudinal component (q_i). The value of r_i obtained appears to be of approximately constant value, independent of the incident beam momentum. This suggests that better separation will be obtained at higher beam momenta simply because the ratio of q_i to r_i will increase.

Fig. 4-1 shows Peyrou plots for the data in this channel (the Peyrou plot is a two dimensional plot of the transverse momenta against the longitudinal momenta in the centre of mass system). These show the justification for the small transverse momenta assumption.

The distribution of events on a θ_1 versus θ_2 plot is shown on Fig. 4-2 which also shows the positions of the face boundaries of the cuboctahedron. The labelling of the regions corresponds to the Feynman diagrams in the previous chapter where the particles with positive values of q are associated with the beam vertex and those with negative values of q with the target vertex.

The θ_1 , θ_2 plot shows several important features.

FIGURE 4-1

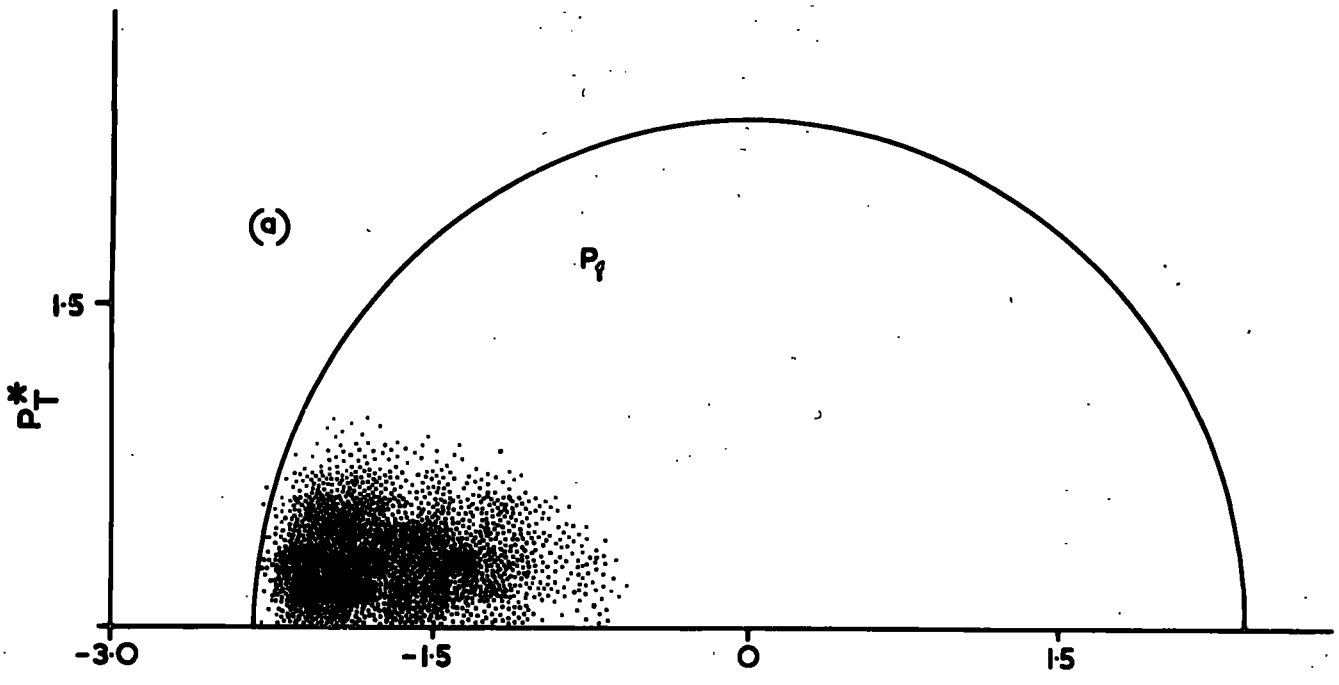

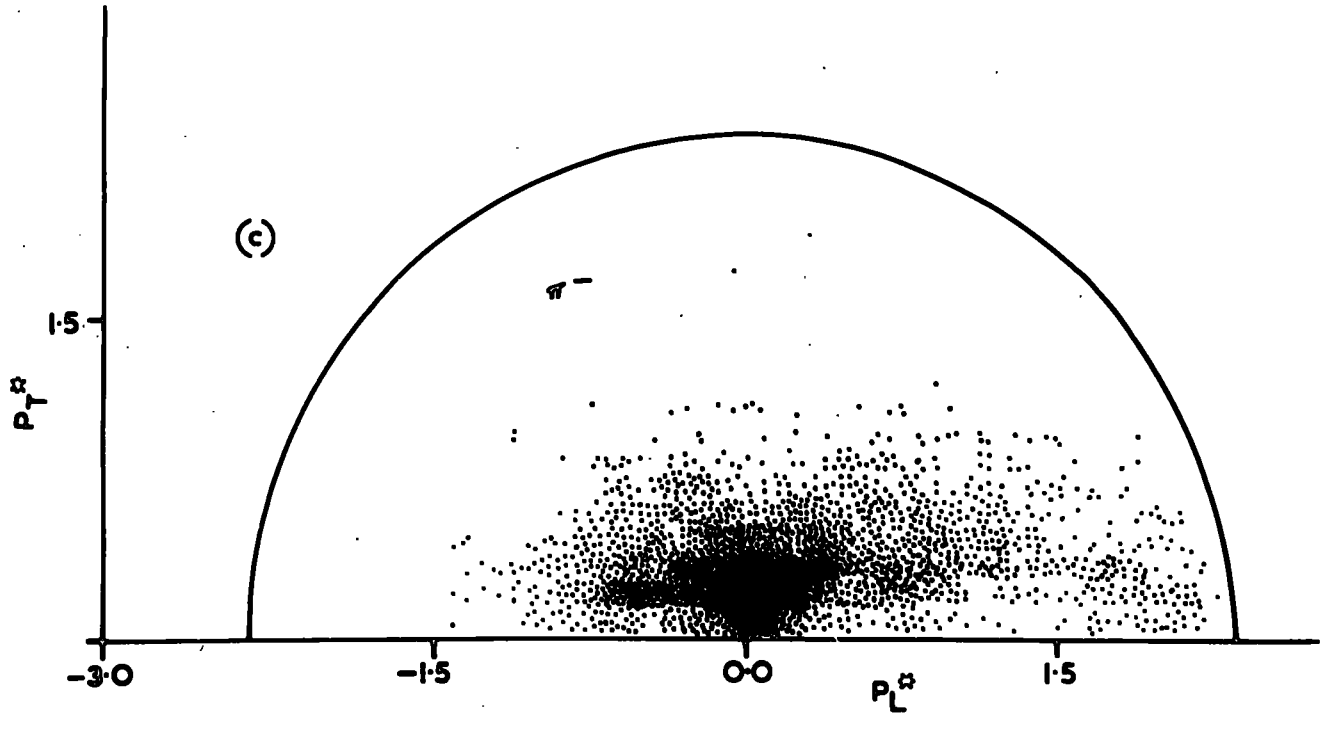

FIGURE 4-1

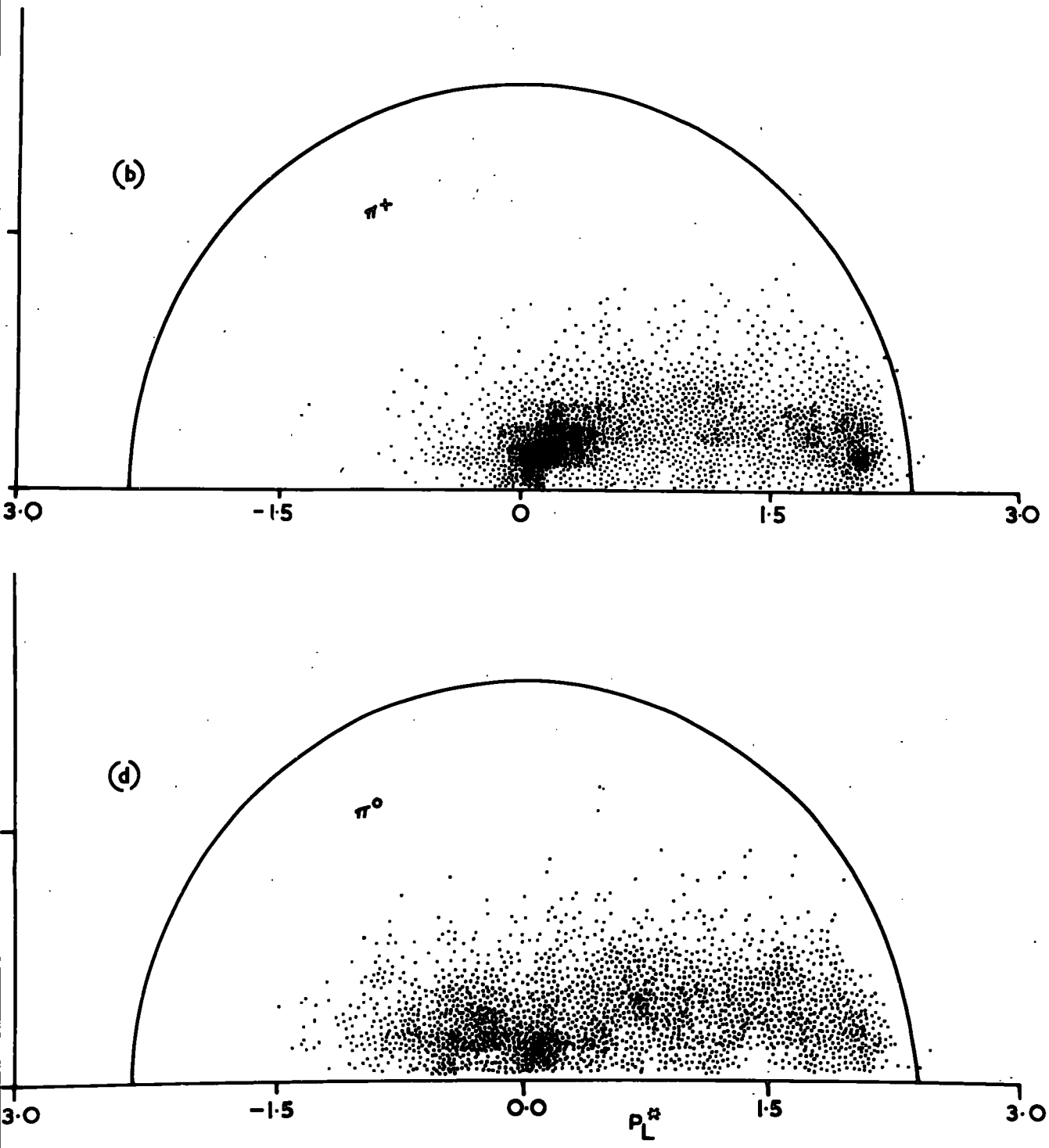

FIGURE 4-2

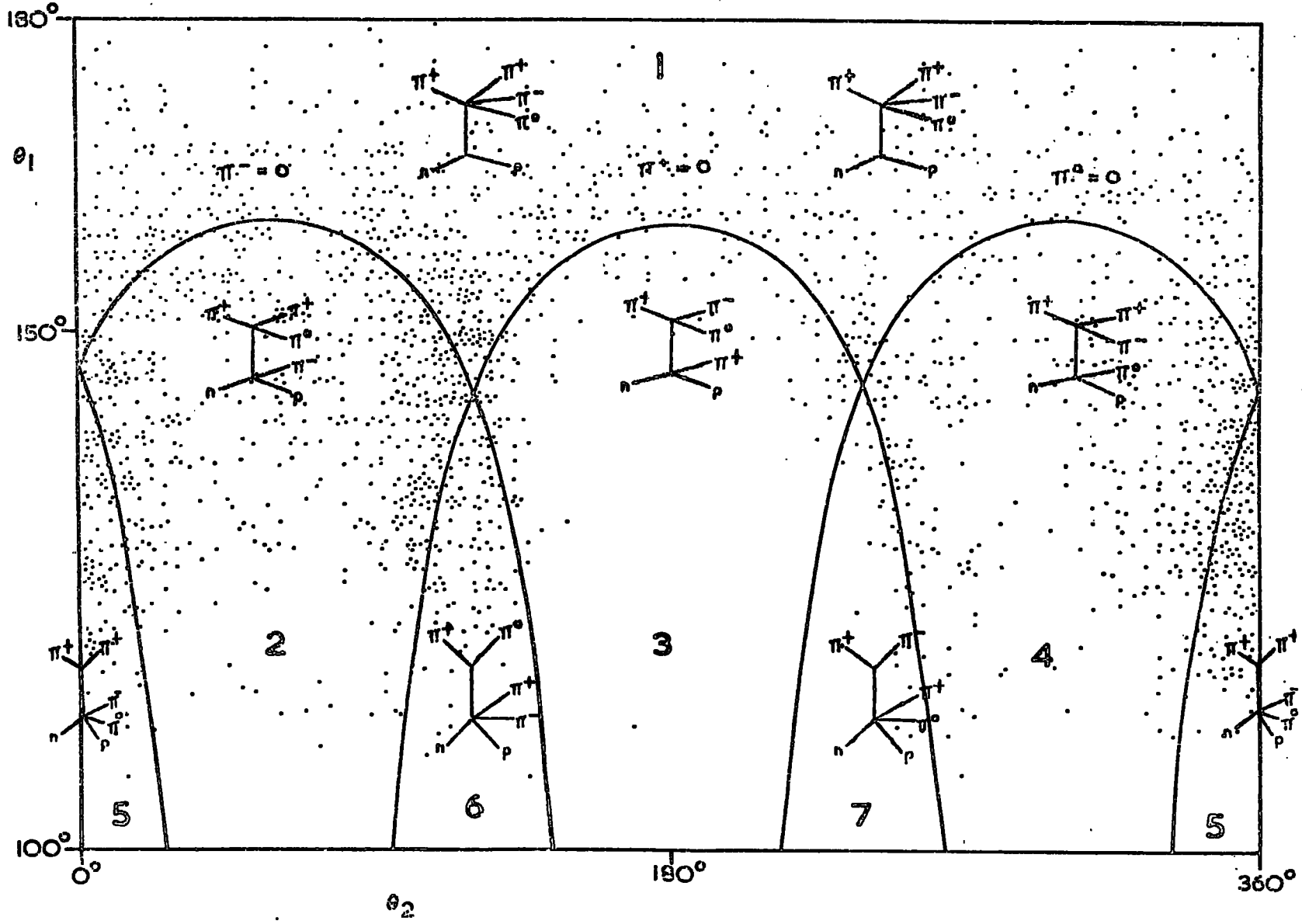

Since all the protons have negative values of q only half the cuboctahedron is populated and so θ_1 need only be considered to vary between 90 and 180 degrees. As would be expected if simple meson exchange dominates, there is a notable lack of events in regions (3) and (7) since these regions correspond to exotic or baryon exchange. Also most of the events in these regions are close to the boundaries shared with simple exchange regions. There is a general clustering close to the boundaries, especially for the negative pion boundary, i.e. where the pion is slow in the centre of mass system. (This is also reflected in the Peyrou plot, Fig. 4-1(C)).

4.1. Tripion Invariant Mass Spectrum in Region (1)

Clearly the regions which are most likely to be of interest are (1), (2) and (4) for tripion and baryon+ dipion resonances. Fig. 4-3 shows the tripion mass spectrum for events in Region (1). Comparison with Fig. 2-8(A) shows that no events with an invariant mass below about 900 MeV/c^2 have been rejected and relatively few have been removed up to a mass value of about 1300 MeV/c^2. However above this value there is increasingly heavy rejection, as would be expected if all the pions are constrained to be moving forwards in the centre of mass system. This selection alone therefore does not remove any background from under

FIGURE 4-3

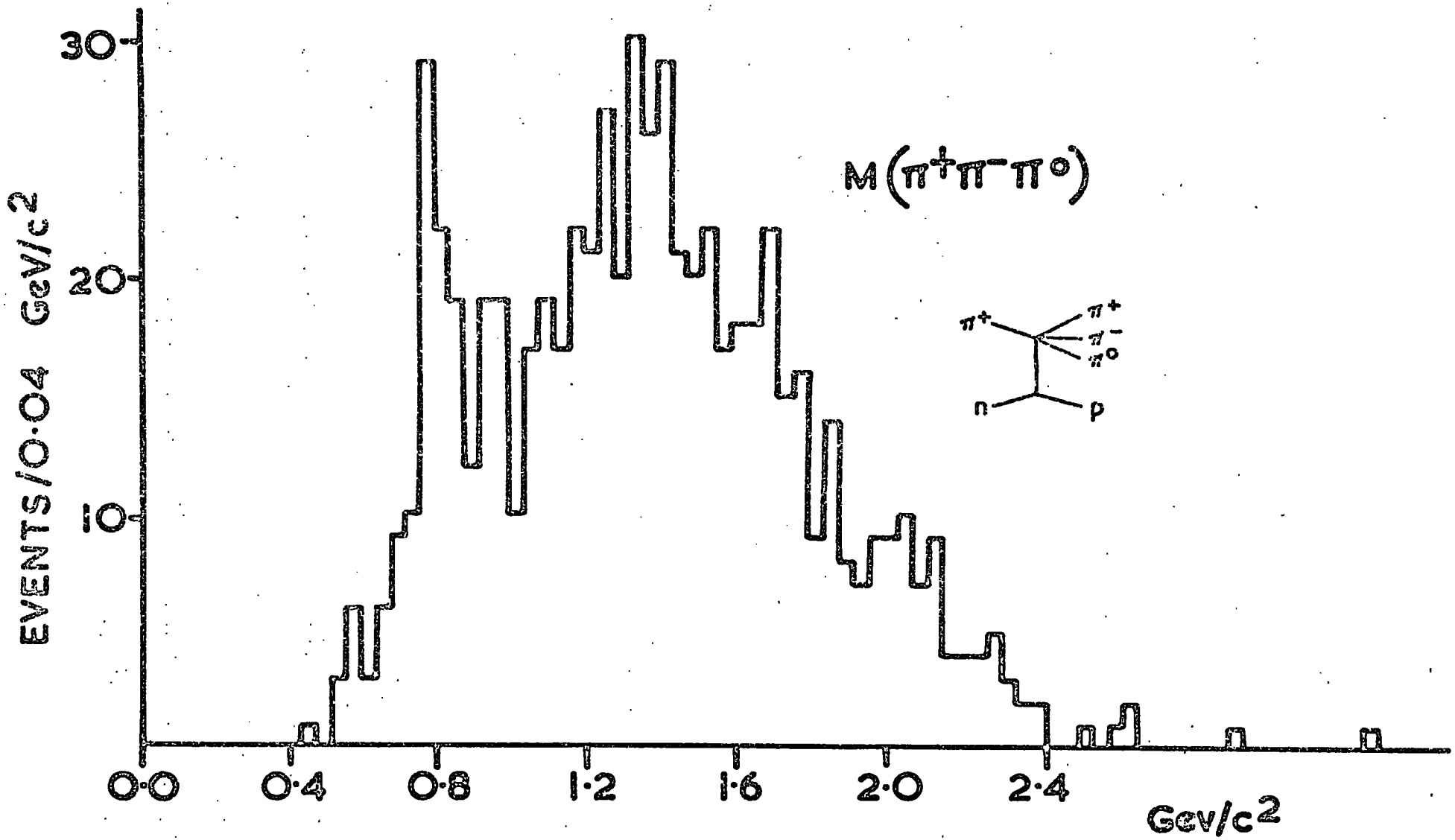

the ω^0 and also does not separate other possible resonances (e.g. A_1^0 , H(990))from the total sample. It does however mean that ω^0 reflections are removed from samples which do not include this region.

The only other possible three pion enhancement in Region (1) corresponds to a mass of just under 1000 MeV/c^2. Although an enhancement (the H(990)) has been seen in several experiments, the existence of a resonance is in considerable doubt. (Ref. 8). In previous experiments $\rho\pi$ decay has been observed with approximately equal contributions from the three ρ charge states. While not being at all stastically significant, it is interesting that the number of possible H(990) events above a hand drawn background corresponds to the number of $\rho\pi$ events in the mass region with approximately equal contributions from the three charge states.

4.2 The $M(p\pi^-)$ and $M(\pi^+\pi^0)$ Spectra in Region (2)

For region (2) the $M(p\pi^-)$ and $M(\pi^+\pi^0)$ mass distributions are shown in Fig. 4-4(A) and (B). The $M(p\pi^-)$ distribution shows the Δ^0 signal on a considerably reduced background. Comparison with Fig. 2-7(A) suggests that a large proportion of the Δ^0 signal is present in this region although the uncertain background makes the exact determination of the effect of the selection difficult. The $M(\pi^+\pi^0)$ spectrum seems to be considerably improved over the full sample

FIGURE 4-4

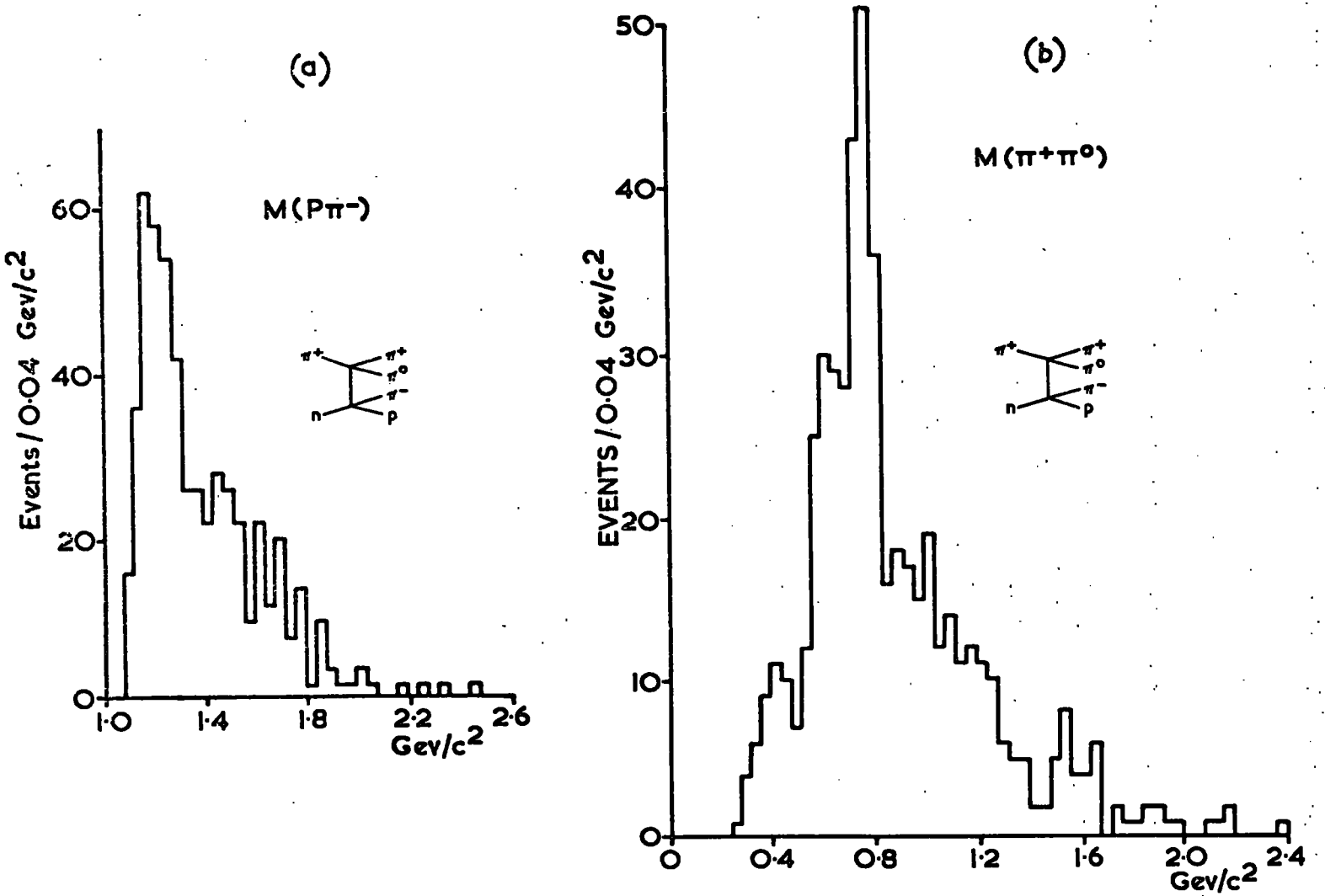
(a)
M(Pπ⁻)
Events / 0·04 Gev/c²
60
40
20
0
1·0
1·4
1·8
2·2
2·6
Gev/c²
π⁺
n
π⁺
π⁰
π⁻
p
(b)
M(π⁺π⁰)
EVENTS / 0·04 Gev/c²
50
40
30
20
10
0
0·4
0·8
1·2
1·6
2·0
2·4
Gev/c²
π⁺
n
π⁺
π⁰
π⁻
p

spectrum shown in Fig. 2-6(B) especially in the signal to the background ratio. However, it would appear that a number of ρ^+ events do not fall in this region and the shoulder at about 600 MeV/c^2, although reduced, is still present. This shoulder does not appear to represent the effect of any other resonance production, and is present in both three prong and four prong data.

4.3. The $M(p\pi^o)$ and $M(\pi^+\pi^-)$ Spectra in Region 4

The $M(p\pi^o)$ and $M(\pi^+\pi^o)$ Spectra corresponding to Region (4) are displayed in Fig. 4-5. The adverse effect of combining the proton with the unmeasured π^o as opposed to the measured π^- can be seen by comparison of the Δ signals in Fig. 4-4(A) and 4-5(A). The Δ^+ is wider and of poorer shape which suggests that the apparent enhancements at higher $p\pi^o$ masses are not significant. As expected there is considerably more Δ^o production than Δ^+ production.

The $M(\pi^+\pi^-)$ mass distribution for Region (4) displays a strong ρ^o signal on a very low background, especially when compared with the full sample (Fig.2-6(B)). The resonance has a good Breit Wigner shape and has no indication of shoulders. There is still an indication of enhancement between 1000 and 1400 MeV/c^2 but the details are not clear.

4.4. The $M(\pi^+\pi^-)$ Spectrum in Region (2)

The $M(\pi^+\pi^-)$ Spectrum for Region (2) is shown in

FIGURE 4-5

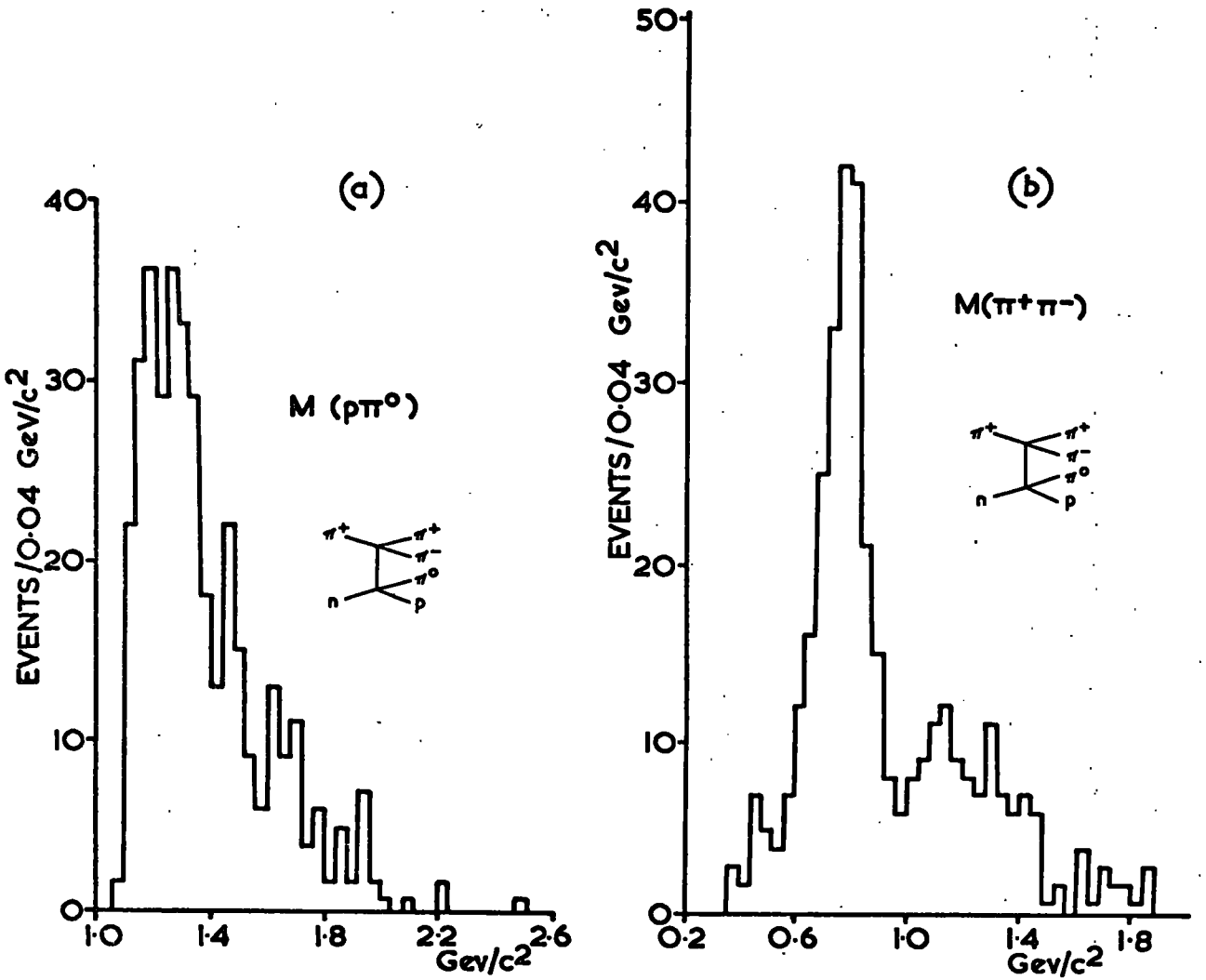
(a)
M (pπ°)
EVENTS/0·04 GeV/c²
40
30
20
10
0
1·0
1·4
1·8
2·2
2·6
Gev/c²
(b)
M(π⁺π⁻)
EVENTS/0·04 Gev/c²
50
40
30
20
10
0
0·2
0·6
1·0
1·4
1·8
Gev/c²

Fig. 4-6(A) and the rather poor ρ^0 signal shown corresponds to the best resonance signal found in an "incorrect" L.P.S. region.

4.5 Discussion of Dipion Spectra for Region (1)

Other resonance signals can be seen in two particle subsets from L.P.S. regions where three particles travel in the same direction in the centre of mass (or rather they have the same sign for their q.s) Perhaps the most important case of this are the three dipion combinations which correspond to Region (1). The invariant mass distributions for the three combinations are shown in Fig. 4-6(B), (C) and (D). The anti-selection of ω^0 simply removes the inevitable reflections of the tripion resonance, which distort the low mass phase space of the dipion systems, and does not materially affect the distributions in the ρ mass regions. All three distributions show a suggestion of ρ production together with a high background the ρ^+ being the most inconclusive. The size of the ρ^+ and ρ^- signals suggest that there is small, if any, A_1^0 production ($A_1^0 \rightarrow \rho^{\pm} \pi^{\mp}$). However, although it is quite possible for a ρ produced from a tripion system not to appear in Region (1) (because of the internal energy of the system), it is not likely that a ρ which should really appear in another region to be tagged as Region (1) event, except by measurement errors. Thus there is likely to be a net loss of ρ

FIGURE 4-6

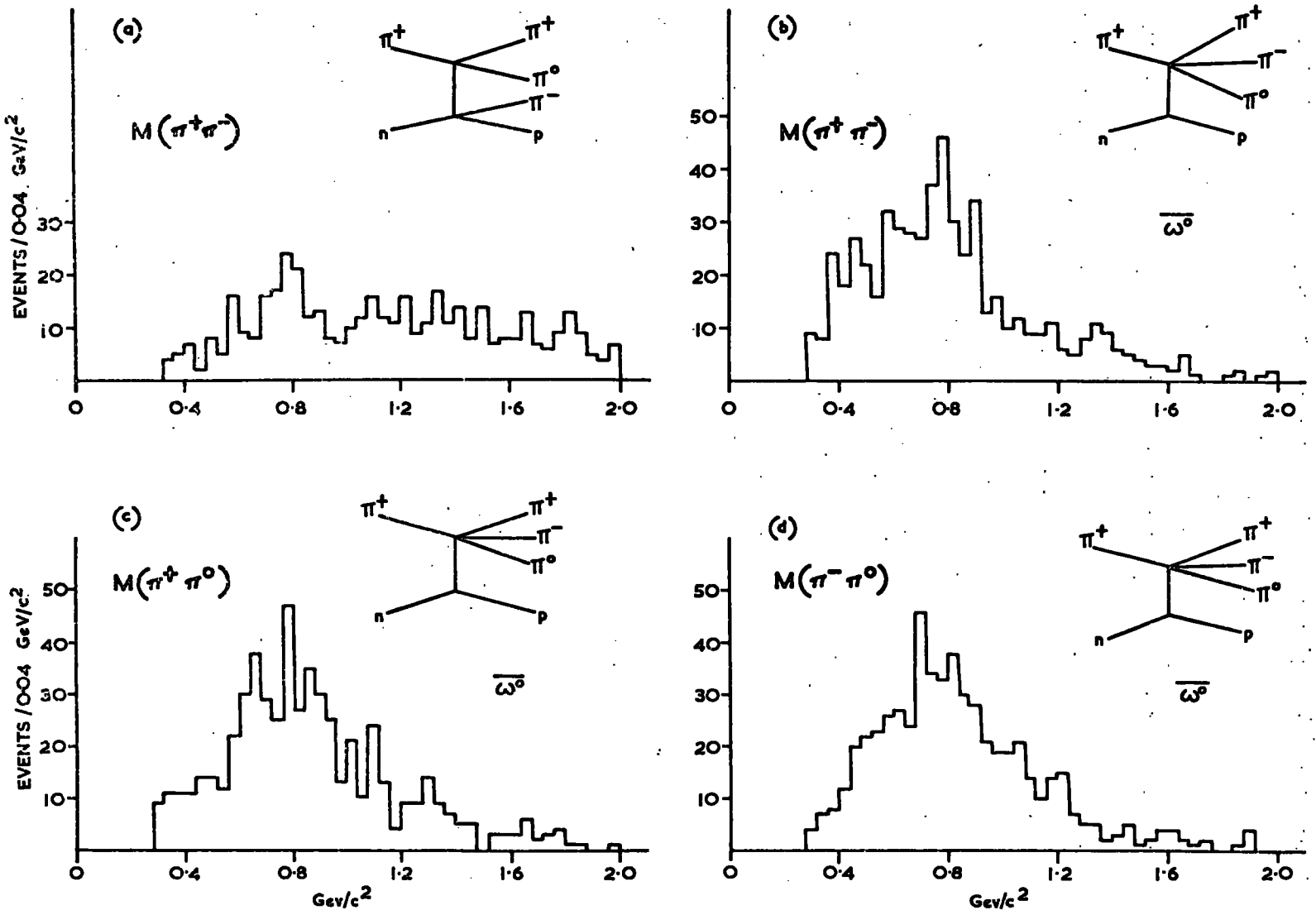
(a)
M(π⁺π⁻)
EVENTS/0·04 GeV/c²
(b)
M(π⁺π⁻)
ω°
(c)
M(π⁺π°)
ω°
EVENTS/0·04 GeV/c²
Gev/c²
(d)
M(π⁻π°)
ω°
Gev/c²

events from Region (1).

Due to the high background level under the ρ signals it is found that most events in Region (1), apart from those events with $M(\pi^+\pi^-\pi^0) \lesssim 800$ MeV/c^2, have at least one dipion combination near a mass region. Perhaps because of this the $M(\pi^+\pi^-\pi^0)$ spectrum for charged ρ events does not display any significant enhancement in the A_1^0 region, since the ρ selection will include considerable background.

4.6 The 'Δ' Signals in Region (5)

In Region (5) there is found to be enhancement in both the $M(\rho\pi^-)$ and $M(\rho\pi^0)$ spectra in the Δ mass region. Both signals have good resonance shapes, but, as can be seen in Fig. 4-7, the same events are contributing to both signals. It is not clear as to whether the signals are purely a kinematic effect or if the production of one Δ constrains the system to the other Δ mass region.

It should be noted that the events in Region (5) correspond almost entirely to the 'leading' pions mentioned previously.

FIGURE 4-7

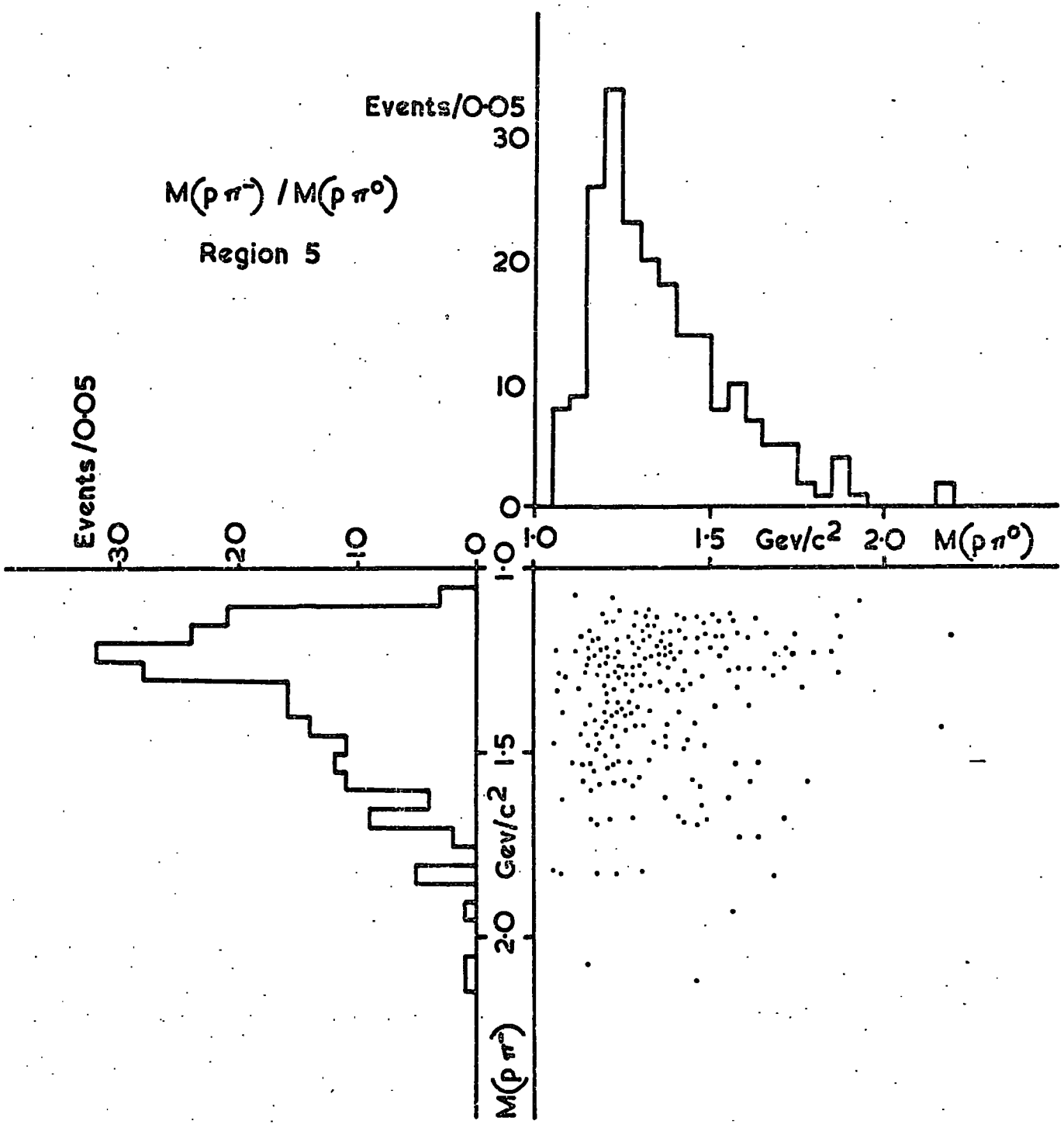
Events/0·05
30
20
10
0
M(p π⁻) / M(p π⁰)
Region 5
Events/0·05
30
20
10
0
1·0
1·5
Gev/c²
2·0
M(p π⁰)
1·0
1·5
2·0
Gev/c²
M(p π⁻)

4.7 Conclusion

The aim of using an analysis system, such as the one suggested by Van Hove, is to facilitate the separation of resonances and specific kinematic configurations from a sample of data. As particle accelerator energies increase, higher multiplicity final states are being analysed more frequently and systematic methods of analysis have increasing advantages over the more conventional analysis methods.

The selection of a particular Van Hove region has a similar effect to an admittedly complex combination of conventional mass and momentum transfer selections. For this reason it is expected that distortion of momentum transfer and angular decay distributions of resonances may occur. This is balanced by the systematic nature of the analysis in that the whole sample is analysed in one operation and an overall picture of the data sample can be obtained.

For the particular data sample described in this Thesis the most striking overall result of Van Hove analysis is the very high level of correspondence between the predictions of the simple Feynman diagrams and the type of events in the appropriate regions. This is shown by the almost complete lack of resonance signals in 'incorrect' regions.

Specifically, while the analysis does not appear to

improve the tripion resonances, it proves effective for the ρ^0 and $\Delta(1236)$ resonances which correspond to a considerable proportion of the total sample. The other notable success is the separation of the 'leading pion' events. The separation of these events does not correspond to purely selecting events with high π^+ momenta since the π^+ momentum distribution with these events removed extends to the kinematic momentum limit, with a shape similar to that of the π^0 momentum distribution.

For this data sample, the Van Hove analysis method has proved effective in separating most low mass resonances and clearly displays the advantages of systematic analysis methods. Since this technique can be very easily applied, it can be used, at the very least, for preliminary analysis of data.

CONCLUSION

The first part of this thesis has described briefly the procedures used to obtain a final sample of about 2000 events fitting the reaction $\pi^+ d \rightarrow p_s p \pi^+ \pi^- \pi^\circ$. This sample was obtained by selection from an original sample of about 7000 fits. The rejected 5000 fits do not contain any significant enhancements corresponding to the above 1c reaction. The total cross-section for the channel has been calculated by another part of the collaboration (ref.2), from which a 2000 event sample implies a microbarn equivalent of 2.4 ± 0.1 events/microbarn.

Using this final sample several features of the data were presented in Chapter 2. There is clear evidence for Δ°, Δ^+, ρ°, ρ^+, ω° and η° resonances, although most of these signals are observed on a fairly large background. The possibility of higher mass N^* resonances and also $\Delta^\circ \rho^+$ and $\Delta^+ \rho^\circ$ associated production was also noted. While there is an accumulation of events in the f° mass region the distribution does not have a resonance shape.

Although the 4 prong events clearly provide a better sample, the improved statistics obtained by including the 3 prong events suggested an

investigation of the larger errors involved in 3 prong events as compared with 4 prong events. An account of this is given in Appendix A and the results are summarised in Table 2. This shows that the absence of the spectator proton information has most effect on mass combinations including the π^0 or π^+, while having least effect on combinations involving the fast proton. With this in mind the 3 prong events were retained but continually checked for compatibility with the 4 prong events.

Using the variables defined in Chapter 3, a Van Hove analysis of the data was performed, the results of which are discussed in Chapter 4. Analysis using the θ_1, θ_2 variables has no effect on the low tripion mass distribution which includes the ω^0 and η^0 mesons and does not appear to separate any higher tripion mass resonances. However quite good separation of the Δ^0 and Δ^+ baryons is obtained and the ρ^+ signal is also considerably improved. The separation of the ρ^0 meson is excellent, comparison of figures 2-6(b) and 4-5(B) shows the large reduction in background obtained.

Another interesting feature of the analysis is the separation of the 'leading pion' events into the expected Van Hove region and the accompanying 'double Δ' production.

Perhaps the best test of this type of analysis, however, is to look for resonance signals in 'incorrect' Van Hove regions, i.e. signals which would not be predicted from the corresponding Feynman diagram. There is only one discernible signal of this type which is the rather poor ρ° signal displayed in Fig. 4-6(A).

In conclusion it would appear that the Van Hove method of Analysis can be a powerful technique in separating low mass resonances.

APPENDIX (A)

There is considerable difficulty in making an assessment of the errors introduced in a three prong 1c fit when an unseen spectator proton is included in the GRIND starting values as having zero momentum with relatively large errors. Since the spectator itself is of little interest the most important effects will occur when the unseen π° is involved. However, it is also expected that mass combinations which do not include the π° would also be affected to a certain amount, since the overall fitting errors will be increased relative to a normal 1c fit.

In order to attempt to estimate these errors, some four pronged events were refitted with GRIND in such a way that the seen spectator proton information was ignored and the event fitted as a three prong. This meant that a direct comparison was possible between a four prong event and a three prong 'event' which has identical track information except that the spectator track is 'unseen'. This procedure clearly gives an upper limit to the errors introduced in normal three prong fits since the spectators which are ignored in fitting four prongs as three prongs will have higher momenta than the truly unseen spectators. The results of this procedure clearly show the differences between mass combinations including the π° and those which

do not involve the π^0 . In order to obtain a better idea of the true errors involved, only four prong events where the fitted spectator has a momentum of less than 120 MeV/c were used. The 'error' on a particular mass combination for a particular pair of fits was assumed to be the difference between the original four prong mass and the 'four prong fitted as a three prong' mass. These values, in general, were found to have a gaussian-like distribution, centred near to zero. The values of the error, in most cases, did not appear to have any strong dependance on the value of the original four prong mass combination. The means and standard deviations of the errors for some of the mass combinations are shown in Table 2.

TABLE 2

The Results of Refitting 4 Prong Events as 3 Prong 'Events' assuming Gaussian-Like Distributions for the 'Errors'

Parameters of Distributions / Mass Combinations	Mean (MeV/c^2)	Standard Deviation (MeV/c^2)
$\pi^+\pi^-$	0.2	3.0
$\pi^+\pi^\circ$	5.0	23.0
$\pi^-\pi^\circ$	4.0	26.0
$\pi^+\pi^-\pi^\circ$	4.0	30.0
$p\pi^-$	1.0	2.0
$p\pi^\circ$	5.0	20.0

REFERENCES

(1) G. E. Pearson Ph.D. Thesis (Durham, 1969)

(2) J. Huc D.E.S. Thesis (Ecole Polytechnique, 1972)

(3) D. Kemp et.al. Lett.al. Nuovo Cimento 2, 471 (1971)

D. Kemp et.al. Nuovo Cimento 8A 611 (1972)

S. M. Scarrott and D. Kemp Lett.al. Nuovo Cimento 3, 271 (1972)

D. Kemp et.al. "Resonance Production in the Reactions $\pi^+ d \rightarrow p_s p \pi^+ \pi^-$ and $\pi^+ d \rightarrow p_s p \pi^+ \pi^- \pi^0$ at 11.7 GeV/c" Submitted to Nuovo Cimento

(4) K. A. Kamakhy Ph.D Thesis (Durham, 1973)

(5) Van Hove Phy.Lett 28B (69) 429
Nuc.Phy. B9, 331 (1969)

(6) Ballam et.al. SLAC PUB-900 May 1971 (TH) and (EXP)

Bartsch et.al. N.P. B19 (1970) 381

Kittel et.al. N.P. B30 (1971) 333

(7) Brau et.al. Phys. Rev. Lett. 27 No. 21 1481 (1971)

(8) For a review of Pre 1968 results see

Fung et.al. Phys. Rev. Lett. 21 No. 46 (1968)

'New' meson seen, Goldhaber quoted by Maglic,

Lund Conference Proceedings P.271 (1969)

ACKNOWLEDGEMENTS

The author wishes to thank Dr. S. M. Scarrott and Mr. D. Kemp for the guidance, assistance and helpful suggestions given at all stages of this work. He would also like to thank Dr. J. V. Major for his interest and help, especially at the later stages of the work. Many thanks are also due to colleagues in the High Energy Nuclear Physics Group and to all other members of the Physics Department for help at various stages of the work.

His thanks are also due to the technical staff of the Physics Department, in particular to Mrs. J. Gibson, Mrs. D. C. Pickles and Mrs. T. Richardson for their help at all times and especially for drawing the figures. The author also wishes to thank the technical and computing staffs of the collaborating laboratories, with a special 'Thank you' to the staff of N.U.M.A.C. and the Durham Computer Unit in particular.

Finally, he also wishes to thank his parents for their encouragement and help, especially his mother who also typed this thesis.

This work has been financed by the Science Research Council.